# Nanoscale

Accepted Manuscript


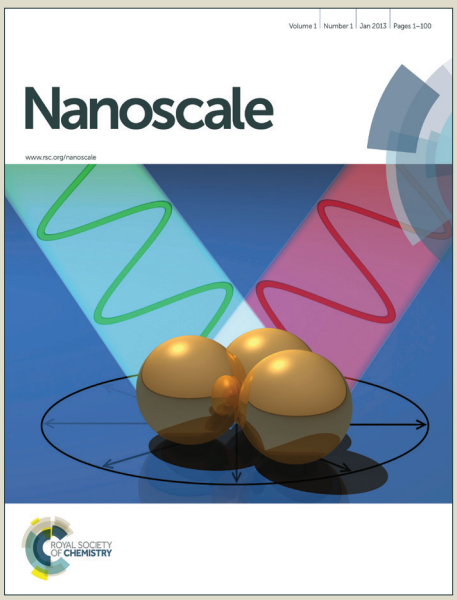





ROYAL SOCIETY OF CHEMISTRY

www.rsc.org/nanoscale

Department of Chemistry
Tianjin University
Tianjin 300072, P. R. China
Tel&Fax: 86-22-27403475
E-mail: bzhang@tju.edu.cn

April 12, 2015

**Re: Manuscript revision-** Manuscript ID NR-ART-01-2015-000607 entitled "Converting 2D Inorganic-organic ZnSe-DETA Hybrid Nanosheets into 3D Hierarchical Nanosheet-based ZnSe Microspheres with Enhanced Visible-light-driven Photocatalytic Performances".

Dear Prof. Chen,

Thank you very much for your handling our manuscript (Manuscript ID NR-ART-01-2015-000607).

According to the reviewer's kind comments and wise suggestions, we have carefully revised the manuscript. With regard to the specific concerns of the referee, we would like to explain them in detail, as shown in a separate response for the reviewers.

To save the reviewer and editor's valuable time, key revisions are highlighted by a yellow background in the revised manuscript.

We thank for all kind comments and wise suggestions from the reviewers. We are sure that the quality of this work will be greatly improved according to these nice comments and wise suggestions from the reviewers.

We hope the revised manuscript meets the criteria of "***Nanoscale***" in its new form. If there are any problems, please feel free to let me know.

Thank you very much.

Regards

Sincerely yours,

Bin Zhang

Department of Chemistry
Tianjin University
Tianjin 300072, P. R. China
Tel&Fax: 86-22-27403475
E-mail: bzhang@tju.edu.cn

# Specific Response

## To Referee 1:

**1. Comments:** This manuscript reported morphology control and Visible-light-driven Photocatalytic Performances of ZnSe Microspheres. There are many similar papers published on morphology control, and the prepared ZnSe Microspheres exhibit weak photocatalytic activity. So I feel that this paper is not suitable for publication in Nanoscale.

**Answer:** We do acknowledge the referee's comments. I don't agree with the reviewer' opinion on "similar papers". Here, we would provide our claims:

1) Recent developments have enabled the chemical transformation of one crystalline material into another desired target material. Three of the most important methods for chemical transformation are ion-exchange reaction, the Kikendall effect and stabilizer-depleted binary semiconductor nanocrystals. As demonstrated in these reported chemical transformation strategies, no dramatic macro-sized morphology transformation during the chemical reaction (e.g. nanowire is transformed into another nanowire, nanodisk is transformed into target nanodisk, sphere is transformed into spherical targets.). The available method including ion-exchange strategy can not solve the challenge that "the 2D morphology into 3D hierarchical transformation." In this manuscript, we realized the transformation of two-dimensional (2D) nanosheets into three-dimensional (3D) hierarchical structures. This chemical transformation strategy from 2D inorganic-organic hybrid nanosheets into 3D hierarchical products can be considered as a new addition to the growing toolbox of "conversion chemistry" reactions.
2) Nanoscale chemical reactivity forms an important basis form any characteristics of nanomaterials ranging from catalytic efficiency to structural transformations. Our work is helpful for understanding the stability and transformation of nanoscale inorganic-organic hybrids, one of important materials with wide applications, in chemical environmental.
3) Although many papers have been published on morphology control of ZnSe, there're still several challenges. Firstly, these reported methods are focused on the surfactants-modulated

Department of Chemistry
Tianjin University
Tianjin 300072, P. R. China
Tel&Fax: 86-22-27403475
E-mail: bzhang@tju.edu.cn

synthesis, in which high-temperature calcinations or surfactants are required. However, we mainly focuses on the engineering transformation of two-dimensional (2D) nanosheets into 3D hierarchical structure at relatively mild conditions, which may contribute to the production of complex 3D hierarchical inorganic nanostructures. Furthermore, we conducted the photocatalytic degradation of methyl orange (MO) under the irradiation of visible light (λ > 420 nm), which is different from those under the irradiation of UV light (*Chem. Eur. J.* 2007, 13, 7926; *J. Phys. Chem. C* 2008, 112, 17095). The photocatalytic efficiency of ZnSe is traditionally negligible in the absence of the UV irradiation (*Chem. Eur. J.* 2011, 17, 8663). We reported relatively high visible-light photocatalytic activity, especially for hydrogen evolution.

Thus, we think it is suitable for being considered in ***Nanoscale***.

## To Referee 2:

Referee Letter: This manuscript reports preparation and photocatalysis of ZnSe nanosheets hierarchically forming a flower-like morphology. Although similar morphology of semiconductor materials have often been reported, the authors indicate fairly high visible-light photocatalytic activity especially for hydrogen evolution, and discuss the mechanism of the morphological control. Thus, the manuscript merits publication in Nanoscale. However, some major revisions are necessary.

**1. Comments:** Experimental method (page 2)

The authors used $Na_2S$ and $Na_2SO_3$ as the sacrificial reagents. However, photocatalysis of metal chalcogenides usually suffers from photocorrosion. The presence of sulfide anions in the reaction solution can change the equilibrium of photocorrosion to somewhat suppress the catalyst dissolution or repair the corroded photocatalysts. If these reactions take place, the

Department of Chemistry
Tianjin University
Tianjin 300072, P. R. China
Tel&Fax: 86-22-27403475
E-mail: bzhang@tju.edu.cn

additives cannot be said simply "sacrificial reagent".

**Answer:** We agree with the referee's kind comments and wise suggestions. We agree with the referee's comments. Though it conventionally regards $Na_2S$ and $Na_2SO_3$ as a mixed sacrificial agent to scavenge the photogenerated holes on the photocatalysis of metal chalcogenides (*Chem. Soc. Rev.* 2009, 38, 253), it do change the equilibrium of photocorrosion and suppress, to a certain extent, the catalyst dissolution as the role of stabilizer (*J. Phys. Chem. C* 2011, 115, 6149). So we add this role of $Na_2S$ and $Na_2SO_3$ in the revised manuscript.

**2. Comments:** Effect of the organic content (page 4, left to right)

Although the authors judge the effect of organic content on the basis of the experiments with different rinsing numbers, such consideration is too qualitative. Organic content in the products should be provided. Also, concentration of DETA in the hydrothermal solutions should be measured. Moreover, the authors do not clearly indicated the effect of $N_2H_4$. At least, the results in the presence of $N_2H_4$ and absence of DETA should be presented.

**Answer:** We do appreciate the referee's kind comments and wise suggestions. Firstly, organic contents in the precursors and in the products are convinced using TGA on a NETZSCH STA 409 analyzer with a ramp rate of 10 ˚C/min from room temperature to 450 °C at $N_2$ atmosphere (Figure. R1 and Figure S2 in the revised Electronic Supplementary Information). The decomposition of ZnSe precursor begins at 150 °C and ends at about 350 °C, with total weight loss of 25.3% ZnSe precursor. The calculation based on the TGA result identify the ZnSe precursor as ZnSe-$(DETA)_{0.5}$, which is consistent with previous report. (W. Yao, S.-H. Yu, X. Huang, J. Jiang, L. Q. Zhao, L. Pan and J. Li, *Adv. Mater.* 2005, 17, 2799–2802.). As for the 3D hierarchical ZnSe products, the organic content in the products is negligible because there's no obvious weight loss in this range. Secondly, the concentration of DETA in the hydrothermal solutions is measured using the UV-vis absorbance spectra. We test a standard UV-vis absorption spectrum of DETA and then analyze the concentration of DETA in the hydrothermal solutions. In the synthesis of hierarchical nanosheet-based ZnSe microspheres ("ZnSe-DETA nanosheets (about 3.4 mL) were dispersed into 16 mL DIW"), the concentration of DETA is 0.1

Department of Chemistry
Tianjin University
Tianjin 300072, P. R. China
Tel&Fax: 86-22-27403475
E-mail: bzhang@tju.edu.cn

mL in the solution. In the synthesis of ZnSe nanoparticles ("0.3 mmol purified ZnSe-DETA nanosheets were dispersed into 16 mL DIW"), the concentration of DETA is almost zero in the solution.

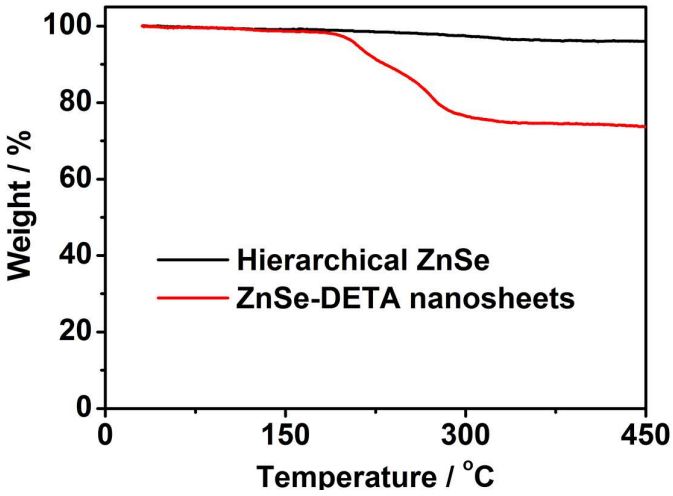


**Figure R1** TGA curves of 3D hierarchical ZnSe products (black line) and ZnSe precursor (red line).

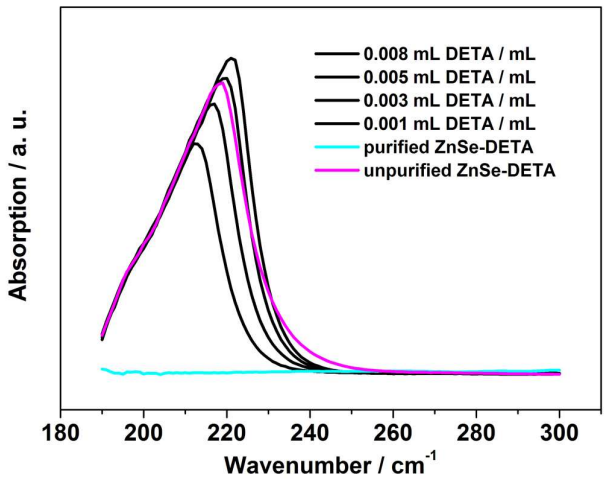


**Figure R2** UV-vis absorbance spectra of DETA standard solutions(black) and the solutions for the synthesis of hierarchical nanosheet-based ZnSe microspheres (magenta line) and ZnSe nanoparticles (cyan line).

According to the reviewer's suggestions, the results in the presence of $N_2H_4$ and absence of

Department of Chemistry
Tianjin University
Tianjin 300072, P. R. China
Tel&Fax: 86-22-27403475
E-mail: bzhang@tju.edu.cn

DETA should be presented. The aggregation of nanoparticles was obtained in the presence of $N_2H_4$ and absence of DETA (Figure R3 and Figure S3c, d, in the revised Electronic Supplementary Information).

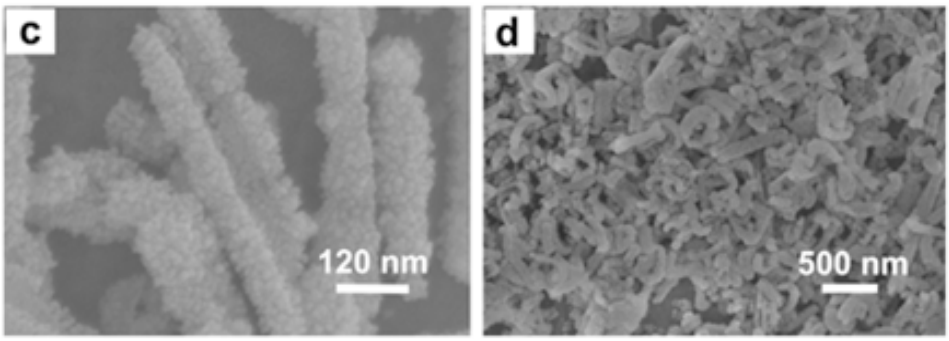


**Figure R1.** SEM images of nanoparticle arrayed ZnSe (c, d) obtained by introducing $N_2H_4{\cdot}H_2O$ (0.8 mL) in the absence of DETA in the reaction system.

**3. Comments:** Formation mechanism (Scheme1)

Although the authors seem to assume topotactic transformation of the precursor to the final ZnSe flowers. However, the results suggest dissolution-recrystallization mechanism because the XRD indicates featureless diffractograms suggesting the formation of an amorphous phase during the morphological transformation.

**Answer:** We do agree with the referee's comment. The transformation of the precursor to the final ZnSe flowers is not exactly topotactic transformation. We found that the peaks of the precursor became weaker and then the peaks of the products became stronger without the co-existence of these peaks in XRD patterns (Figure R4 and Figure 4g in the revised manuscript), suggesting that the transformation do not occur via a topotactic process. Based on our observation on the intermediates, we proposed the dissolution-recrystallization mechanism.

Department of Chemistry
Tianjin University
Tianjin 300072, P. R. China
Tel&Fax: 86-22-27403475
E-mail: bzhang@tju.edu.cn

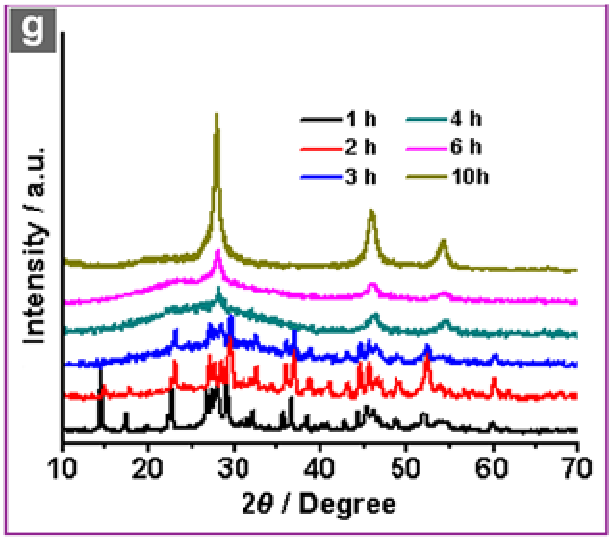


**Figure R4** XRD patterns (g) of the intermediates collected after the transformation reaction proceeded for different times: a) 1 h, b) 2 h, c) 3 h, d) 4 h, e) 6 h, f) 10 h.

**4. Comments:** Photocatalysis (page 6)

The author should provide fundamental characterizations such as surface area and durability of the photocatalytic particles. The UV-vis spectrum of the ZnSe flower (Fig. 6c) indicates different absorption profile around the absorption edge from conventional ZnSe particle. The authors should comment the reason for this and relationship to the photocatalytic activity.

**Answer:** We do appreciate the referee's kind comments and wise suggestions. Firstly, we add the surface area of ZnSe microspheres and ZnSe nanoparticles using the Brunauer-Emmett-Teller method (Figure R5 and Figure S8, in the revised Electronic Supplementary Information). Hierarchical nanosheet-based ZnSe microspheres display the surface area of 55.163 $m^2 g^{-1}$, which is larger than that of ZnSe nanoparticles (37.563 $m^2 g^{-1}$).

Department of Chemistry
Tianjin University
Tianjin 300072, P. R. China
Tel&Fax: 86-22-27403475
E-mail: bzhang@tju.edu.cn

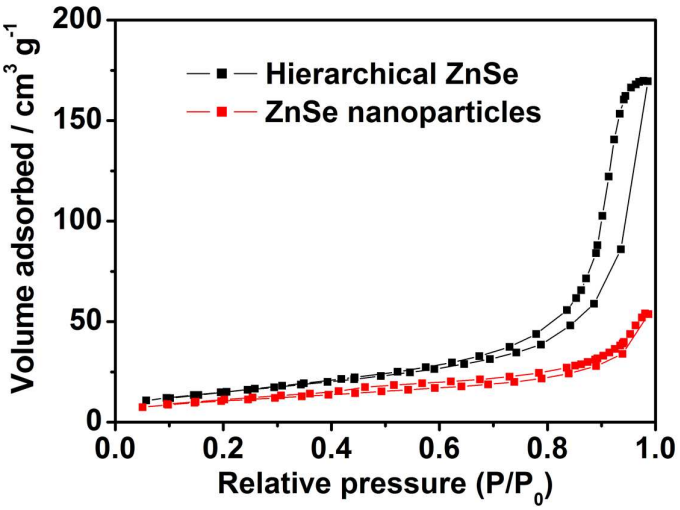


**Figure R5** $N_2$ adsorption isotherm curves of hierarchical nanosheet-based ZnSe microspheres (black line) and ZnSe nanoparticles (red line).

According to the reviewer's kind suggestions, the morphologies of the ZnSe flower and ZnSe particle after the the photocatalytic hydrogen evolution are characterized by the SEM images (see Figure R6 and Figure S9 in the revised Electronic Supplementary Information). No obvious change in their morphology is observed after the 12 h photocatalytic test, indicating their good durability.

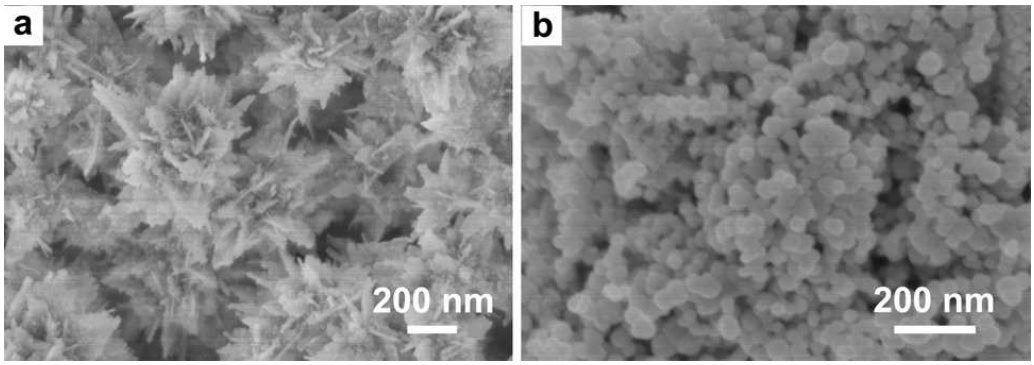


**Figure R6.** SEM images of the ZnSe flower and the ZnSe particle after the the photocatalytic reaction.

The UV-vis spectrum of the ZnSe flower (Fig. 6c) indicates different absorption profile around the absorption edge from conventional ZnSe particle. As shown in the UV-vis absorption spectra of the published work on ZnSe nanostructures (*Chem. Mater.* 2005, 17, 1296), the band

Department of Chemistry
Tianjin University
Tianjin 300072, P. R. China
Tel&Fax: 86-22-27403475
E-mail: bzhang@tju.edu.cn

gap of ZnSe experienced red shifts when the nanostructures changed from sphere (0D) to nanorod (1D), or when the length of nanorods was increased. Similarly, the as-prepared ZnSe flower has the 3D hierarchical nanosheet-based spherical morphology, which is quite different from conventional ZnSe particle (0D). So, the absorption profile of our 3D hierarchical nanosheet-based ZnSe microspheres is different from those of the reported nanopartice and nanorods. Furthermore, the multiple scatter in the hierarchical ZnSe microspheres may enhance the absorbance of photons and further change the absorption profile. We add this comment in the revised manuscript.

We appreciate all kind and wise suggestions from the reviewer 2. We are sure that the quality of this work will greatly improved from these nice comments and wise suggestions from reviewer 2.

## To Referee 3:

Referee Letter: This paper reports the synthesis of the hierarchical assembly of ZnSe nanosheets and the visible light photocatalytic activity of the resulting materials. The synthesis is novel and the obtained materials are well-characterized, which merits the publication of this paper in Nanoscale.

However, there are several issues to be addressed before the acceptance of this paper.

**1. Comments:** What is the content of organic residue in the final product? The role of organic residue in the photocatalytic activity of ZnSe should be discussed. Information of chemical composition should be provided with TGA, ICP, etc.

**Answer:** We do appreciate the referee's kind comments and wise suggestions. Firstly, organic contents in the precursors and in the products are convinced using TGA on a NETZSCH STA 409 analyzer with a ramp rate of 10 ˚C/min from room temperature to 450 °C at $N_2$ atmosphere (Figure. R1 and Figure S2 in the revised Electronic Supplementary Information). The

Department of Chemistry
Tianjin University
Tianjin 300072, P. R. China
Tel&Fax: 86-22-27403475
E-mail: bzhang@tju.edu.cn

decomposition of ZnSe precursor begins at 150 °C and end at about 350 °C, with total weight loss of 25.3% ZnSe precursor. The calculation based on the TGA result identify the ZnSe precursor as ZnSe-$(DETA)_{0.5}$, which is consistent with previous report. (W. Yao, S.-H. Yu,* X. Huang, J. Jiang, L. Q. Zhao, L. Pan and J. Li,* *Adv. Mater.* 2005, 17, 2799–2802). As for the 3D hierarchical ZnSe products, the organic content in the products is negligible because there's no obvious weight loss in this range.

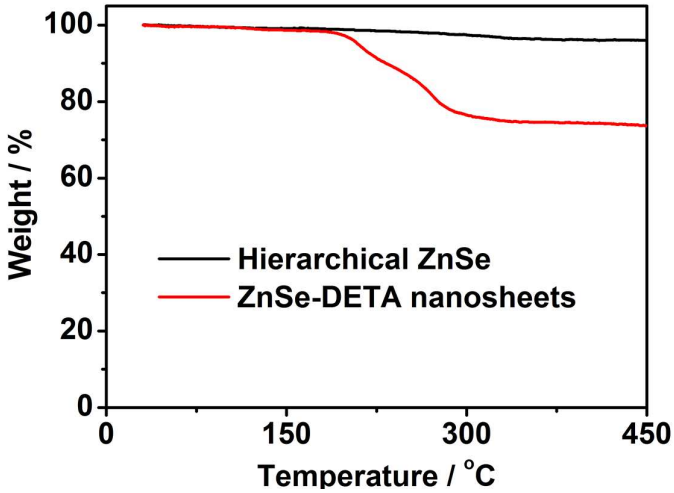


**Figure R1** TGA curves of 3D hierarchical ZnSe products (black line) and ZnSe precursor (red line).

**2. Comments:** Surface area has profound effect on the photocatalytic activity of nanostructured materials. BET characterization is demanded.

**Answer:** We do appreciate the referee's kind comments and wise suggestions. According to the kind suggestions of two reviewers, we add the surface area of ZnSe microspheres and ZnSe nanoparticles using the Brunauer-Emmett-Teller method (Figure R2 and Figure S8, in the revised Electronic Supplementary Information). Hierarchical nanosheet-based ZnSe microspheres display the surface area of 55.163 $m^2 g^{-1}$, which is larger than that of ZnSe nanoparticles (37.563 $m^2 g^{-1}$).

Department of Chemistry
Tianjin University
Tianjin 300072, P. R. China
Tel&Fax: 86-22-27403475
E-mail: bzhang@tju.edu.cn

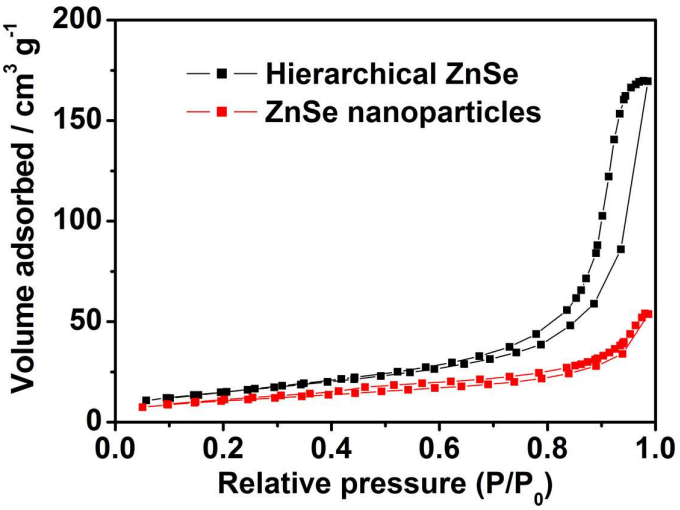


**Figure R2** $N_2$ adsorption isotherm curves of hierarchical nanosheet-based ZnSe microspheres (black line) and ZnSe nanoparticles (red line).

**3. Comments:** Information of the local structural variation of ZnSe upon the 2D-> 3D transformation would be helpful for the readers.

**Answer:** We agree with the referee's kind comments and wise suggestions. So we add the local structural variation of ZnSe upon the 2D-> 3D transformation (Figure R3 and Figure 4a,c in the revised manuscript) as the supplement of the morphology transformation processes. As shown in Figure R3a, at the early stage of the reaction, the release of the DETA molecules between the layers of the ZnSe-DETA hybrid precursors (2D) results a few wall-like embryonic products on the ZnSe-DETA hybrid precursors(3D). In Figure R3c, some walls (2D) in the embryonic products were dissolved and intertwined together to generate 3D flower-like rudiments.

Department of Chemistry
Tianjin University
Tianjin 300072, P. R. China
Tel&Fax: 86-22-27403475
E-mail: bzhang@tju.edu.cn

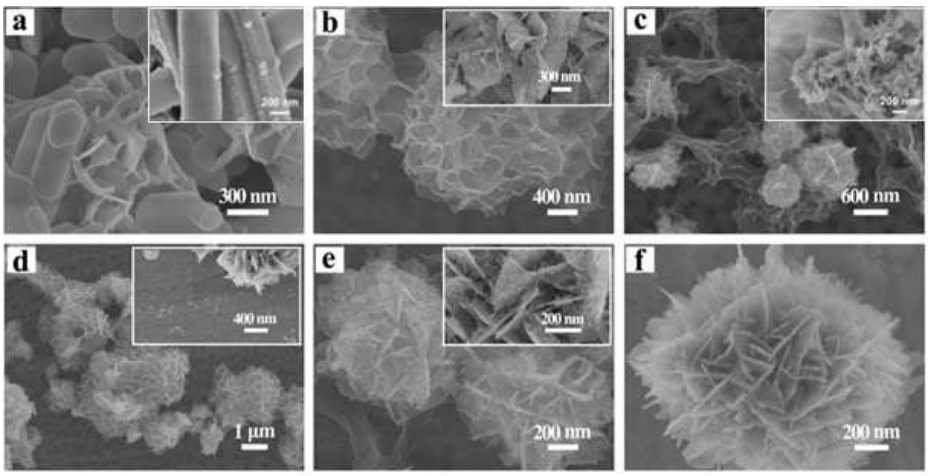


**Figure R3.** SEM images of the intermediates collected after the transformation reaction proceeded for different times: a) 1 h, b) 2 h, c) 3 h, d) 4 h, e) 6 h, f) 10 h.

Finally, we appreciate all kind comments and wise suggestions from the three reviewers. The referee's comments and suggestions are really helpful for us to improve the quality of our manuscript and for our future studies.

Journal Name

RSCPublishing

ARTICLE

# Converting 2D Inorganic-organic ZnSe-DETA Hybrid Nanosheets into 3D Hierarchical Nanosheet-based ZnSe Microspheres with Enhanced Visible-light-driven Photocatalytic Performances

Cite this: DOI: 10.1039/x0xx00000x

Received ooth January 2012,
Accepted ooth January 2012

DOI: 10.1039/x0xx00000x

www.rsc.org/

Xuan Wu,[‡a] Rui Xu,[‡a] Rongjiao Zhu,[*a] Rui Wu[ab] and Bin Zhang[*a]

Engineering two-dimensional (2D) nanosheets into three-dimensional (3D) hierarchical structure is one of the great challenges in nano chemistry and material science. We report a facile and simple chemical conversion route to fabricate 3D hierarchical nanosheet-based ZnSe microspheres by using 2D inorganic-organic hybrid ZnSe-DETA (DETA=diethylenetriamine) nanosheets as the starting precursors. The conversion mechanism involves the controlled depletion of the organic-component (DETA) from the hybrid precursors and the subsequent self-assembly of the remnant inorganic-component (ZnSe). The transformation reaction of ZnSe-DETA nanosheets is mainly influenced by the concentration of DETA in the reaction solution. We demonstrated that this organic-component depletion method could be extended to the synthesis of other hierarchical structures of metal sulfides. Additionally, the obtained hierarchical nanosheet-based ZnSe microspheres exhibited outstanding performance in visible light photocatalytic degradation of the methyl orange and were highly active for photocatalytic $H_2$ production.

## 1. Introduction

Nanostructures with fascinating properties and novel applications in catalysis, gas sensing, photonics, energy storage and bionanotechnology have inspired great increasing efforts to design and control the morphology, structure, and composition of the nanocrystals to optimize the properties of materials.[1-12] Diverse advanced chemical transformation strategies, such as ion-exchange reaction, the Kirkendall effect and stabilizer-depleted approaches, have been developed to convert one starting material into another desired target material which cannot be easily prepared by other methods.[13-17] Recently, we have developed a facile ion-exchange and organic component stripping strategy of inorganic-organic hybrid nanowires or nanosheets to fabricate hierarchical porous $MoS_2$ nanotubes or $Cd_xZn_{1-x}Se$ hollow nanoframes.[18-19] And unary porous single-crystal-like semiconductor Te nanoplates could be generated from binary materials through an organic compound assistant depletion method.[20] In particular, stabilizer-depleted method, which based on the removal of the organic stabilizer and the spontaneous self-assembly of the individual inorganic building blocks, has emerged as a charming strategy for the synthesis of nanomaterials with tunable morphology and even more complex structures as well as unique properties.[21] At present, most of these researches were mainly focused on the transformation from nanoparticles to the nanowires by the action of the stabilizer. For example, Se and Te nanowires resulted from the interesting spontaneous reorganization of their binary semiconductor nanoparticles have been investigated in detail.[22, 23] This stabilizer-depleted method can also be utilized for the preparation of nanowires from noble metals.[24] Additionally, the *in situ* self-assembly of the nanoparticles via the partial removal of the organic stabilizer can also be used for the synthesis of some other shaped nanomaterials.[13, 25] Oil-phase synthesis of some crystalline nanoflowers via the limited ligand protection strategy has been previously studied by Peng group.[26] Yu and co-workers have reported that hybrid nanobelts can be transformed into inorganic nanotubes due to the release of the stabilizer in the selected organic solvents.[27] Despite of these progresses in stabilizer-depleted synthesis of nanomaterials, the production of three-dimensional (3D) hierarchical inorganic nanostructures via the depletion of the organic component from inorganic-organic hybrid nanosheets has not been adequately developed.[28]

Hierarchical structures composed of diverse nanocrystals have attracted worldwide attention owing to their unique properties and widespread potential applications in various fields, which are different from and even surpass their primary structures.[4, 29-38] For instance, Lou and co-workers demonstrated that hierarchical nanostructures owned the

fascinating performance in energy conversion and storage.[31-33] Currently, a wide range of strategies such as self-assembly of the primary building blocks or template-assisted fabrication, chemical vapor deposition, electron irradiation and bottom-up growth method have been developed to fabricate semiconductor nanocomposites with hierarchical nanostructures.[39-42] As one of the most well-known II–VI semiconductor materials, ZnSe, with a direct band gap of 2.67 eV and excellent optoelectronic properties, has been widely studied for the promising photovoltaic applications.[43-48] However, the development of a facile and universal approach to synthesize 3D hierarchical nanosheet-based ZnSe micromaterials on large scale for the photocatalytic application is still in its infancy.

Herein, we report a facile and effective way to prepare 3D hierarchical ZnSe microspheres via the depletion of organic component of unpurified inorganic–organic 2D ZnSe–DETA hybrid nanosheets. It has been shown that nanosheet-based ZnSe microspheres can be synthesized by tuning the concentration of DETA in the reaction solution. Moreover, this organic-component depletion method of hybrid nanosheets may be also suitable for fabricating hierarchical sphere-like nanostructures of other sulfides and selenides. The subsequent performance test shows that the as-prepared inorganic hierarchical ZnSe microspheres with the mixture of single-crystalline and twinning structure exhibit enhanced performance in the photocatalytic degradation of methyl orange (MO) and photocatalytic hydrogen production.

## 2. Experimental section

### 2.1. Chemicals

All chemicals are analytical grade and were used as received without further purification. Aqueous solutions were prepared using deionized water (DIW).

### 2.2. Synthesis of hybrid ZnSe-DETA and ZnS-DETA nanosheets.

Inorganic-organic hybrid nanosheets were prepared as our previously reported method.[17]

### 2.3. Synthesis of hierarchical nanosheet-based ZnSe microspheres.

For the synthesis of inorganic hierarchical nanosheet-based ZnSe microspheres, 0.3 mmol unpurified ZnSe-DETA nanosheets (about 3.4 mL) were dispersed into 16 mL DIW under vigorous stirring, then the mixture was transferred into 20 mL Teflon-lined stainless-steel autoclave and kept at 150 °C for 12 h, and cooled down naturally. The resultant yellow products were collected by centrifuging and washed with absolute ethanol and DIW for several times to remove any possible remained amine, and then dried under a vacuum at 40 ºC for 6 h for further use.

### 2.4. Synthesis of hierarchical nanosheet-based ZnS microspheres.

The procedure for the synthesis of inorganic ZnS 3D hierarchical microspheres is the same to that of ZnSe microspheres except that the ZnSe-DETA nanosheets were replaced by ZnS-DETA nanosheets.

### 2.5. Synthesis of ZnSe nanoparticles.

For the synthesis of ZnSe nanoparticles, ZnSe-DETA nanosheets were first rinsed to remove adsorbed $N_2H_4 \cdot H_2O$ and DETA, then about 0.3 mmol purified ZnSe-DETA nanosheets were dispersed into 16 mL DIW under vigorous stirring, the as-prepared dispersion was finally transferred into 20 mL Teflon-lined stainless-steel autoclave and kept at 150 °C for 12 h.

### 2.6. Characterization

The scanning electron microscopy (SEM) images were taken with a Hitachi S-4800 scanning electron microscope (SEM, 3 kV). Transmission electron microscopy (TEM), higher-magnification transmission electron microscopy (HRTEM) images were obtained with JEOL-2100F system. Specimens for TEM and HRTEM measurements were prepared via dropcasting a droplet of ethanol suspension onto a copper grid, coated with a thin layer of amorphous carbon film, and allowed to dry in air. The X-ray diffraction patterns (XRD) of the products were recorded with Bruker D8 Focus Diffraction System using a Cu Kα source (λ= 0.154178 nm). FTIR spectra were recorded on a MAGNA-IR 750 (Nicolet Instrument Co) FTIR spectrometer. UV-vis diffuse reflectance spectra (UV-vis DRS) were recorded on a Lambda 750S UV–vis-NIR spectrometer (Perkin-Elmer) equipped with an integrating sphere. The UV-vis DRS of solid samples were collected in 200–800 nm against $BaSO_4$ reflectance standard. The surface area was determined by nitrogen physisorption using Quadrasorb SII Quantachrome Instrumen and calculated using the Brunauer-Emmett-Teller (BET) method. Thermogravimetric analysis (TGA) was measured by NETZSCH STA 409 analyzer with a ramp rate of 10 ºC $min^{-1}$ from room temperature to 450 °C at the $N_2$ atmosphere.

### 2.7. Photocatalytic degradation of methyl orange

The photocatalytic activities of 3D hierarchical ZnSe microspheres for the degradation of methyl orange (MO) were carried out under visible-light irradiation. For each test of MO degradation, 30 mg catalyst power was dispersed into 100 mL of $5\times10^{-5}$ M MO solution. A 300 W Xe lamp equipped with a cutoff filter (λ > 420 nm) was used as the optical system. The suspension solution was kept stirring at room temperature for 10 h in the dark to ensure the absorption equilibrium of the water, MO and the catalyst. The distance between the Xe lamp and the reaction solution was about 18 cm. Then the mixture solution was exposed to visible-light irradiation under constantly stirring. A water bath connected to the flowing water was used to keep the whole reaction solution maintain at room temperature. The concentration of MO was analyzed by UV-vis spectrophotometer.

### 2.8. Photocatalytic hydrogen evolution

For the photocatalytic hydrogen production, a 100 mL top-irradiation Pyrex cell reactor and a 300 W Xe lamp equipped with a cutoff filter (λ > 420 nm) were employed. The Pyrex flask was cooled by the flowing water to keep the tests at room temperature. Before exposing to the visible light irradiation, approximately 30 mg catalyst power was dispersed into 50 mL aqueous solution containing 0.5 M $Na_2S$ and 0.5 M $Na_2SO_3$ as the sacrificial reagents and stabilizer, and then the mixture was sonicated for about 5 minutes to prepare homogenous dispersion. The composition of products mixture was analyzed with an on-line Agilent 7890A gas chromatography equipped with a TCD detector.

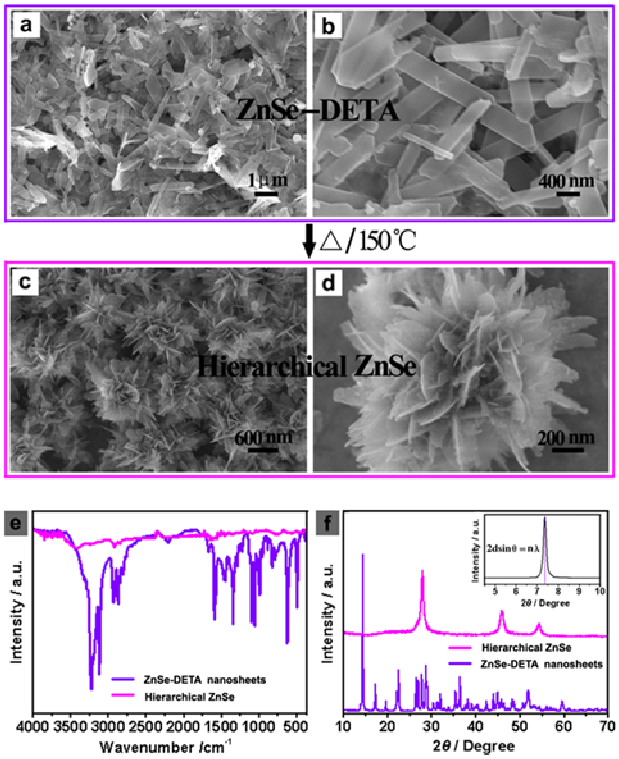


**Figure 1.** (a, b) SEM images of the ZnSe-DETA nanosheets. (c, d) Typical SEM images of the as prepared 3D hierarchical ZnSe microspheres obtained by the hydrothermal transformation of the ZnSe-DETA hybrid nanosheets through the organic-component depletion method. (e) FTIR spectra of the ZnSe-DETA hybrid nanosheets (purple line) and inorganic ZnSe hierarchical microstructures (magenta line). (f) XRD patterns of ZnSe-DETA nanosheets (purple, lower trace), ZnSe hierarchical microspheres (magenta, upper trace) and low-angle XRD pattern of ZnSe-DETA (inset).

## 3. Results and discussion

The ZnSe–DETA nanosheets were prepared using a modified amine-assisted solvothermal method and then used as starting materials to obtain inorganic hierarchical nanosheet-based ZnSe microspheres under the hydrothermal condition. The size and morphology of the hybrid ZnSe–DETA nanosheets were first examined by SEM. Low-magnification SEM image in Figure 1a shows that the ZnSe–DETA nanosheets could be synthesized successfully. High-magnification SEM image demonstrates that these nanosheets possess a thickness of about 80 nm (Figure 1b). FTIR spectrum (Figure 1e) and XRD pattern (Figure 1f) further identify the obtained samples as inorganic-organic hybrid ZnSe-DETA nanosheets. The small angle XRD pattern (the inset of Figure 1f) indicates that these hybrid precursors own the layered structure with an interlayer spacing of about 1.2 nm (calculated by Prague formula). The unpurified ZnSe–DETA nanosheets were then used as the starting materials and hydrothermally treated at 150 °C for 12 h to obtain the products. Representative SEM image shows that the products are uniform spherical structure with diameters of 1 μm (Figure 1c). High-magnification SEM image (Figure 1d) demonstrates that the as-prepared ZnSe microspheres are hierarchical architectures of irregular nanosheets. Energy-dispersive X-ray (EDX) spectrum (Figure S1, Supporting Information) displays the samples are composed of pure Zn and Se. The ratio of Zn to Se is ca. 1. FTIR spectra (Figure 1e) suggest the transformation of hybrid ZnSe-DETA precursors to the inorganic hierarchical microstructures. In the typical XRD pattern of the as-converted hierarchical nanosheet-based microspheres (Figure 1f), all the diffraction peaks can be indexed to the wurtzite phase of ZnSe (JCPDS 15-0105), implying that the as-obtained hierarchical microspheres are ZnSe with high purity. Organic contents in the precursors and in the products are analyzed using TGA (Figure S2, Supporting Information). The decomposition of ZnSe precursor begins at 150 °C and ends at about 350 °C, with total weight loss of 25.3%, confirming the molecular formula of inorganic-organic hybrids as ZnSe-$(DETA)_{0.5}$. As for the 3D hierarchical ZnSe products, the organic content in the products is negligible because there's no obvious weight loss in this range.

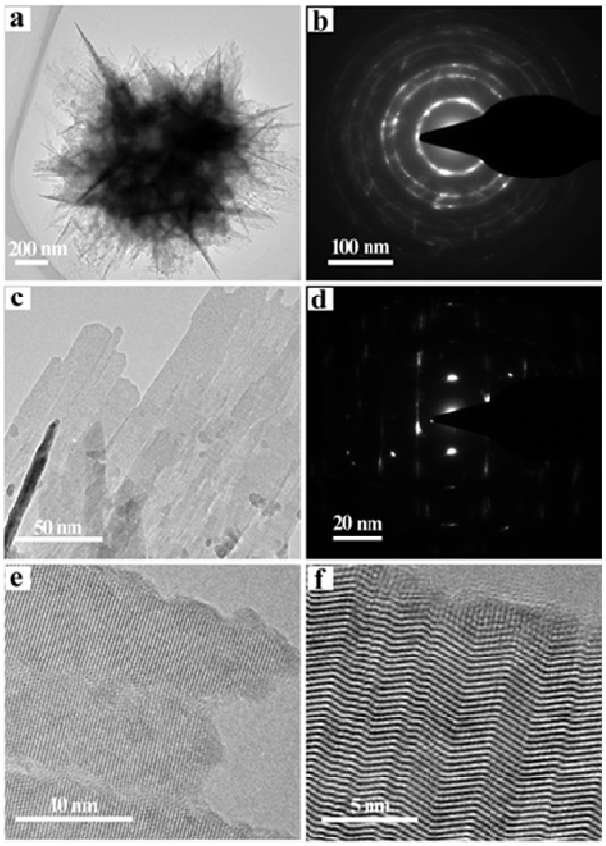


**Figure 2.** (a) TEM image of the ZnSe hierarchical microstructure; (b) corresponding SAED pattern of an individual ZnSe microsphere. (c) TEM image of the individual ZnSe nanosheet, (d) the SAED pattern of the nanosheets which compose the hierarchical structures. (e, f) HRTEM of the ZnSe nanosheets.

The morphology and structure of the hierarchical nanosheet-based ZnSe microspheres were further studied by transmission electron microscopy (TEM), selected area electron diffraction (SAED) and high-resolution TEM (HRTEM). Typical TEM image of the inorganic ZnSe microspheres presented in Figure 2a indicates that these hierarchical structures are composed of irregular nanosheets. The associated SAED pattern of the individual microsphere displayed in Figure 2b confirms that these hierarchical ZnSe structures are polycrystalline. The representative TEM image of the fringe of an individual ZnSe nanosheet (Figure S3, Supporting Information) indicates that the thickness of irregular nanosheets in hierarchical nanosheet-based microspheres is about 5-8 nm. TEM image displayed in Figure 2c further shows that these microspheres are hierarchical architecture of nanosheets. The associated SAED pattern of one main sheet (Figure 2d) and their HRTEM images (Figure 2e, f) show that there exists the mixture of single-crystal-like and twinning superlattice phases in the ZnSe hierarchical microspheres. The appearance of twinning crystal may be attributed to the changes in the selenium fugacity, and such twinning structure may exert a noticeable influence on the optical, electronic and mechanical properties of the as-prepared ZnSe hierarchical microspheres.[49-54] These results testify that inorganic-organic hybrid ZnSe-DETA nanosheets can be successfully transformed into inorganic hierarchical nanosheet-based ZnSe microspheres with the mixed single-crystalline and twinning structure.

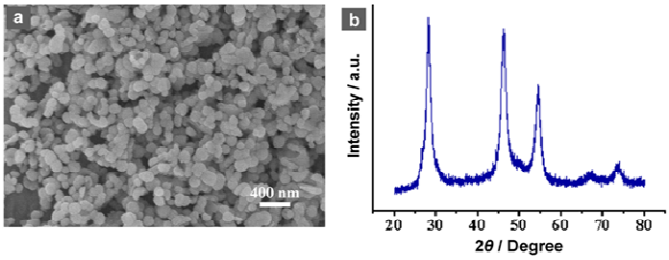


**Figure 3.** SEM image (a) and XRD pattern (b) of the ZnSe nanoparticals.

It should be pointed out that the unpurified ZnSe–DETA nanosheets obtained from the amine-assisted solvothermal method contains the superfluous $N_2H_4 \cdot H_2O$ and DETA. To further explore the formation process, the roles of the $N_2H_4 \cdot H_2O$ and DETA on the structure transformation were studied. When ZnSe-DETA samples were rinsed to completely remove adsorbed $N_2H_4 \cdot H_2O$ and DETA, and were then used as the starting precursors with other conditions unchanged, the products were irregular inorganic wurtzite ZnSe nanoparticles with a diameter of 40-100 nm (Figure 3 and Figure S4a, b, Supporting Information). When rinsed ZnSe-DETA samples were mixed with an appropriate amount of $N_2H_4 \cdot H_2O$ in the absence of DETA and reacted in the same hydrothermal condition, aggregation of nanoparticles was obtained (Figure S4c, d, Supporting Information). These results suggest that DETA plays an important role in the transformation of ZnSe-DETA hybrid nanosheets into inorganic nanosheet-based ZnSe hierarchical structures. We also found that the concentration of DETA in the solution exerted a remarkable influence on the transformation of the hybrid nanosheets. When an appropriate amount of DETA was introduced into the hydrothermal reaction system, ZnSe hierarchical microstructures can also be generated (Figure S5a-d, Supporting Information). However, once excessive DETA ($V_{DETA} \geq 2$ mL) was added, the high concentration of DETA in the solution will hamper the dissolution of DETA from the hybrid nanosheets into the reaction system, and then the transformation from ZnSe-DETA hybrid nanosheets to the hierarchical ZnSe microstructures will be prevented (Figure S5e-f, Supporting Information). Therefore, we can speculate that the concentration of the DETA in the hydrothermal solution plays a key role in the transformation reaction.

We have also found that the reaction temperature and the solvent play important roles in the conversion of inorganic-organic hybrid ZnSe-DETA nanosheets. When DIW was used as the solvent for the transformation reaction at 180 °C, the products generated from the reaction were hierarchical ZnSe microspheres with a size of about 1 μm (Figure S6b, Supporting Information). But, once the reaction temperature is lower than 150 °C, the reaction would be difficult to initiate (Figure S6a, Supporting Information). On the other hand, 3D hierarchical



 

ZnSe microstructures can also be generated when ethylene glycol (EG) was used as the reaction medium, while the transformation process may need to react at higher temperature (more than 180 °C), and the size of obtained structures is around 300 nm (Figure S7, Supporting Information). The solvent has a noticeable influence on the transformation products, which may be associated with the solvability of DETA in different solvents. When the transformation reaction was performed in EG, the reaction needs higher temperature probably due to the slow release of the DETA in the EG solution.

To gain insight into the transformation mechanism of the reaction, the morphology and phase transformation processes were investigated by performing the time-dependent experiments SEM and XRD were used to characterize the intermediates collected at different stages of the reaction. The local structural variations of ZnSe could also know from the SEM images (inset in Figure 4). When the reaction proceeded for 1h, a few wall-like embryonic products were obtained (Figure 4a), which may be generated due to the partial release of the DETA molecules between the layers of the ZnSe-DETA hybrid precursors. The corresponding XRD pattern displayed in Figure 4g revealed that these samples were mainly ZnSe-DETA nanosheets. After the reaction proceeding for 2 h, the thickness of precursor nanosheets decreased while the amount of the embryonic products composed of thin walls increased and some walls were intertwined together to generate the early flower-like products (Figure 4b). If the reaction time was prolonged to 3 h, light yellow product composed of ZnSe flower-like rudiments and semi-finished nanosheets were obtained. The latter can serve as the subsequent resources for the following growth of the ZnSe microspheres (Figure 4c). When the reaction time was increased to 4 h, the individual nanosheets almost disappeared, and the samples mostly became hierarchical ZnSe nanostructures (Figure 4d). The prolonged exchange reaction and the slow dissolution of DETA in water made the middle area of the sheets break into small particles and the edges became bigger and rougher, and a mass of small nanoparticles generated along with the reaction were found in the reaction solution (inset of Figure 4d). After 6 h, the dispersed ZnSe nanoparticles in the solution disappeared and were found to adsorb on the surfaces of the 3D hierarchical ZnSe microspheres, as shown in Figure 4e. As confirmed by XRD patterns in Figure 4g, along with the reaction time, the amount of DETA in the intermediates decreased and the intermediates transformed gradually into inorganic ZnSe hierarchical structures of wurtzite phase. When the reaction is prolonged to 10 h, the small nanoparticles disappeared gradually and recrystallized onto the pre-generated platelets. So the surfaces of the microspheres became more smooth and perfectly transformed 3D hierarchical ZnSe structures were obtained (Figure 4f). Moreover, the phase transformation characterized by XRD pattern in Figure 4g revealed that the signal of the organic component was disappeared and pure wurtzite ZnSe phase was produced.

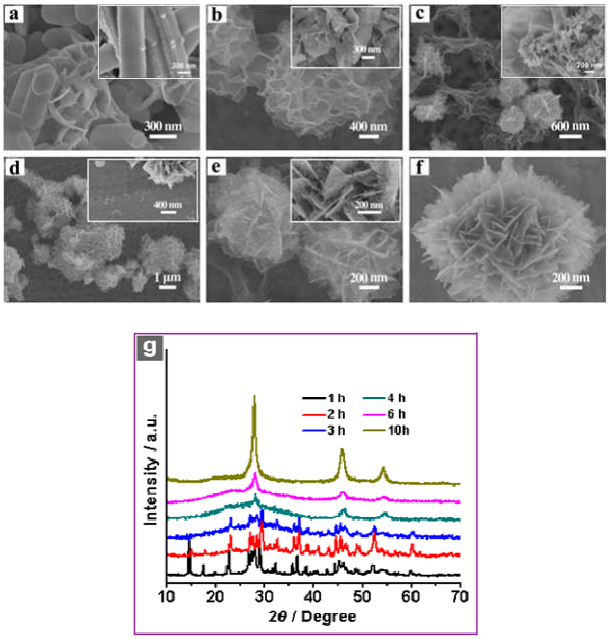


**Figure 4.** SEM images (a-f) and XRD patterns (g) of the intermediates collected after the transformation reaction proceeded for different times: a) 1 h, b) 2 h, c) 3 h, d) 4 h, e) 6 h, f) 10 h.

Organic amine molecules have been reported to play a key role in the fabrication of 2D metal sulfides.[55] Herein, on the base of the above-mentioned results, we propose a DETA-induced nucleation and self-assemble mechanism with following Ostwald ripening process for the chemical conversion of inorganic-organic hybrid ZnSe-DETA nanosheets into inorganic hierarchical nanosheet-based ZnSe microspheres. Firstly, the DETA molecules dissolve gradually from the hybrid precursors into the reaction solution at elevated temperature. Meanwhile, the residual ZnSe components turn into sheet-like embryonic structures via a dissolution-recrystallization process due to the induced role of DETA.[28, 55] Upon prolonging the reaction time, the as-generated sheet-like embryonic structures intertwined together to generate the early flower-like product through a self-assembly process. Finally, with the elongation of reaction time, thermodynamically stable hierarchical nanosheet-based ZnSe microspheres are obtained by the Ostwald ripening growth process (Scheme 1). Note that an additional systematic study is necessary to fully explore fundamental issues of size- and shape-dependent conversion activity for this strategy.

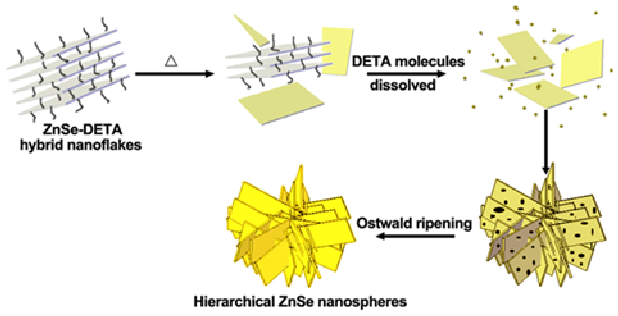


**Scheme 1.** Scheme illustrating the synthesis of inorganic hierarchical ZnSe microspheres through the organic-component depletion method of the unpurified inorganic-organic ZnSe-DETA hybrid nanosheets at 150 ºC.

Given these insights into the reaction that converts inorganic-organic ZnSe-DETA nanosheets to inorganic hierarchical nanosheet-based ZnSe microspheres and consideration of the chemical factors involved in the process, the conversion of other hybrid precursors to inorganic hierarchical structures may be expected. For instance, when unpurified inorganic-organic ZnS–DETA nanosheets were used as the starting materials for the transformation reaction in the hydrothermal solution at 150 °C, inorganic 3D hierarchical ZnS microspheres could also be generated (Figure 5). These results suggested this organic-component depletion triggered transformation reaction method presented herein might be expanded to the synthesis of microsphere-like structures of other metal sulfides and selenides.

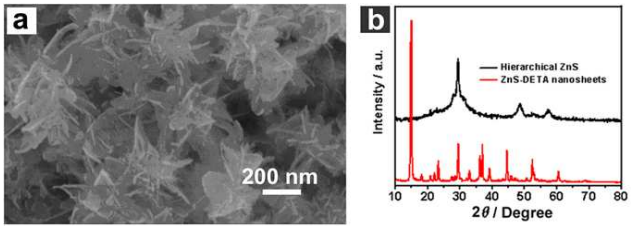


**Figure 5.** a) Typical SEM image of 3D hierarchical ZnS microspheres. b) XRD patterns of ZnS-DETA nanosheets (red line) and inorganic 3D hierarchical ZnS microspheres (black line).

Recently, semiconductor nano- and micron-materials with controlled morphologies and structures have been found to exhibit fascinating photocatalytic activities.[36, 56-60] Despite the advances in the synthesis of ZnSe nano- and micron-structures, the development of ZnSe nanomaterials with unique structures and improved catalytic activities under visible-light irradiation is still rarely reported. Herein, the photocatalytic dye degradation and photocatalytic hydrogen production of hierarchical ZnSe were measured for comparative studies with ZnSe nanoparticles. The photocatalytic activities of ZnSe for the degradation of methyl orange (MO) were carried out under visible-light irradiation ($\lambda > 420$ nm), and in each test, 30 mg catalyst power was utilized for the degradation of 100 mL MO ($5\times10^{-5}$ M) solution. The characteristic absorption peak of MO at 464 nm was measured to deliver the photocatalytic results. Figure 6a, b demonstrate the UV-vis absorption spectral changes of MO solution after the treatment of ZnSe catalysts along with the photocatalytic reaction hours, respectively. The diffuse reflectance UV-vis spectra of ZnSe nanoparticles and hierarchical fractal ZnSe nanospheres are presented in Figure 6c, indicating that the as-prepared hierarchical ZnSe possess improved photon capture ability compared to the ZnSe nanoparticles. The absorption profile of the hierarchical fractal ZnSe microspheres differs from the conventional ZnSe nanoparticles, which may arise from the morphology difference from 0D to 3D structure and the multiple scatter in the 3D hierarchical ZnSe microstructures. Figure 6d shows the degradation curves of MO in water under visible light irradiation in the presence of ZnSe catalysts, which clearly show that the degradation of MO is up to 97.1% after treatment by the hierarchical nanosheet-based ZnSe catalyst for 4h, while for the ZnSe nanoparticles it is only 39.6%.

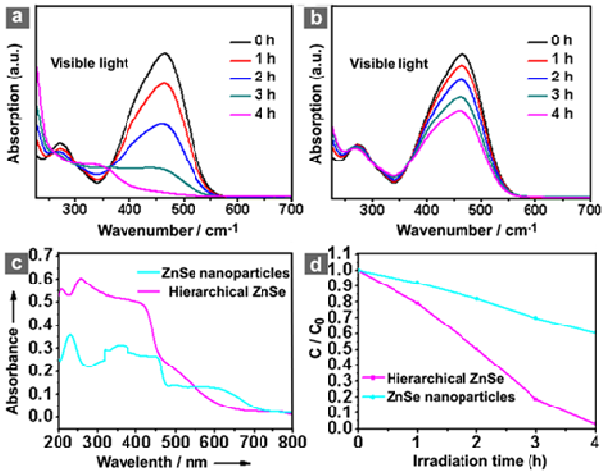


**Figure 6.** UV-visible absorption spectra for MO solutions under visible light in the presence of hierarchical fractal ZnSe (a) and ZnSe nanoparticles (b); (c) diffuse reflectance UV-vis spectra of ZnSe nanoparticles and 3D hierarchical ZnSe microspheres; (d) photobleaching curves of MO under visible light over ZnSe nanoparticles and 3D hierarchical ZnSe microstructures.

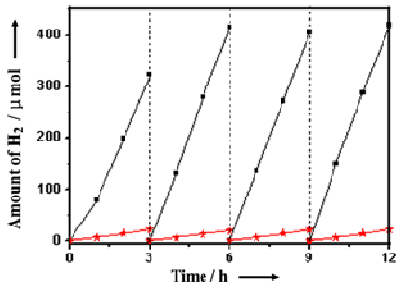


**Figure 7.** Time courses of $H_2$ evolution under the irradiation of visible-light of the as-prepared hierarchical nanosheet-based ZnSe microspheres (black, ■) and ZnSe nanoparticles (red, ★).

Furthermore, we have found that the as-prepared hierarchical nanosheet-based ZnSe microspheres exhibit enhanced catalytic performance for the photocatalytic hydrogen evolution under the irradiation of visible light. The surface area of ZnSe microspheres and ZnSe nanoparticles is characterized

using the BET method. As shown in Figure S8, hierarchical nanosheet-based ZnSe microspheres display the surface area of 55.163 $m^2 g^{-1}$, which is larger than that of ZnSe nanoparticles (37.563 $m^2 g^{-1}$). Figure 7 displays the reaction time courses for $H_2$ evolution under visible light over 3D hierarchical ZnSe microspheres and ZnSe nanoparticles. As shown in Figure 7, the photocatalytic reaction on hierarchical ZnSe microstructures exhibits a stable $H_2$-release rate of approximately 135 μmol $h^{-1}$ per 0.3 g of catalyst, which is about 18 times higher than that of ZnSe nanoparticles. The morphology stability of hierarchical ZnSe microstructures and ZnSe nanoparticles after the photocatalytic hydrogen evolution is identified by the SEM images (Figure S9, Supporting Information), which indicate their good durability. These results suggest that the as-prepared hierarchical ZnSe microspheres exhibit enhanced photocatalytic performance than ZnSe nanoparticles. This improved photocatalytic performance may be associated with the twinning structure of the ZnSe hierarchical nanosheets, which has enhanced the optical transitions to improve the photocatalytic performance.[53, 54] Additionally, the 3D hierarchical ZnSe microstructures lead to more active sites and higher stability of the catalysts.[61-63]

## 4. Conclusions

In summary, we have demonstrated a convenient organic-component depletion approach for the synthesis of inorganic hierarchical nanosheet-based ZnSe microspheres by utilizing the unpurified hybrid ZnSe-DETA nanosheets as the raw materials and treating them in the hydrothermal solution. The time-dependent morphology and phase conversion processes revealed that the transformation mechanism involving the slow dissolution of DETA, the following DETA-induced self-assembly process and the final Ostwald ripening growth. We also showed that this organic-component depletion method of inorganic-organic hybrid microstructures could be extended to the synthesis of other 3D hierarchical metal sulfides. In addition, the as-prepared hierarchical nanosheet-based ZnSe microspheres showed enhanced performances in visible light photocatalytic activities for both dye degradation and $H_2$ production.

## Acknowledgements

This work was financially supported by the National Natural Science Foundation of China (21422104 and 21373149) and the Innovation Foundation of Tianjin University.

## Notes and references

[a] *Department of Chemistry, School of Science, Tianjin University, and Collaborative Innovation Center of Chemical Science and Engineering (Tianjin), Tianjin, 300072, P. R. China. Fax&Tel: +86-22 27403475; E-mail: bzhang@tju.edu.cn (B. Z.) zhurongjiao@tju.edu.cn (R. Z.)*

[b] *School of Chemical Engineering and Technology, Tianjin University, Tianjin, 300072, P. R. China.*

† Electronic Supplementary Information (ESI) available: supplementary Figures: Figure S1–9. See DOI: 10.1039/b000000x/

‡ These authors contributed equally to this work.

1. M. A. Dobrovolskaia and S. E. McNeil, *Nature Nanotech.*, 2007, **2**, 469-478.
2. C.-H. Cui, H.-H. Li, J.-W. Yu, M.-R. Gao and S.-H. Yu, *Angew. Chem. Int. Ed.*, 2010, **49**, 9149-9152.
3. K. Zhou and Y. Li, *Angew. Chem. Int. Ed.*, 2012, **51**, 602-613.
4. S. Deng, V. Tjoa, H. M. Fan, H. R. Tan, D. C. Sayle, M. Olivo, S. Mhaisalkar, J. Wei and C. H. Sow, *J. Am. Chem. Soc.*, 2012, **134**, 4905-4917.
5. H. Zhang and H. Cui, *Nanoscale*, 2014, **6**, 2563-2566.
6. Y. Liu and Z. Tang, *Adv. Mater.*, 2013, **25**, 5819-5825.
7. Y. Zhu, C. Cao, S. Tao, W. Chu, Z. Wu and Y. Li, *Sci. Rep.*, 2014, **4**.
8. J. W. Hong, S.-U. Lee, Y. W. Lee and S. W. Han, *J. Am. Chem. Soc.*, 2012, **134**, 4565-4568.
9. S. Sun and Z. Yang, *Chem. Commun.*, 2014, **50**, 7403-7415.
10. M. Chen, B. Wu, J. Yang and N. Zheng, *Adv. Mater.*, 2012, **24**, 862-879.
11. Y. Wang, Y. Bai, X. Li, Y. Feng and H. Zhang, *Chem. Eur. J.*, 2013, **19**, 3340-3347.
12. Y. Mai, F. Zhang and X. Feng, *Nanoscale*, 2014, **6**, 106-121.
13. Z. Tang, Y. Wang, S. Shanbhag, M. Giersig and N. A. Kotov, *J. Am. Chem. Soc.*, 2006, **128**, 6730-6736.
14. D. H. Son, S. M. Hughes, Y. Yin and A. P. Alivisatos, *Science*, 2004, **306**, 1009-1012.
15. Y. Yin, R. M. Rioux, C. K. Erdonmez, S. Hughes, G. A. Somorjai and A. P. Alivisatos, *Science*, 2004, **304**, 711-714.
16. Y. Yu, X. Yin, A. Kvit and X. Wang, *Nano Lett.*, 2014, **14**, 2528-2535.
17. Y. Yu, J. Zhang, X. Wu, W. Zhao and B. Zhang, *Angew. Chem. Int. Ed.*, 2012, **51**, 897-900.
18. S. Zhuo, Y. Xu, W. Zhao, J. Zhang and B. Zhang, *Angew. Chem. Int. Ed.*, 2013, **52**, 8602-8606.
19. X. Wu, Y. Yu, Y. Liu, Y. Xu, C. Liu and B. Zhang, *Angew. Chem. Int. Ed.*, 2012, **51**, 3211-3215.
20. H. Zhang, H. Wang, Y. Xu, S. Zhuo, Y. Yu and B. Zhang, *Angew. Chem. Int. Ed.*, 2012, **51**, 1459-1463.
21. Z. Tang, Y. Wang, S. Shanbhag and N. A. Kotov, *J. Am. Chem. Soc.*, 2006, **128**, 7036-7042.
22. Z. Tang, N. A. Kotov and M. Giersig, *Science*, 2002, **297**, 237-240.
23. Z. Tang, Y. Wang, K. Sun and N. A. Kotov, *Adv. Mater.*, 2005, **17**, 358-363.
24. Y. Sun, B. Mayers, T. Herricks and Y. Xia, *Nano Lett.*, 2003, **3**, 955-960.
25. Z. Tang, P. Podsiadlo, B. S. Shim, J. Lee and N. A. Kotov, *Adv. Funct. Mater.*, 2008, **18**, 3801-3808.
26. A. Narayanaswamy, H. Xu, N. Pradhan and X. Peng, *Angew. Chem. Int. Ed.*, 2006, **45**, 5361-5364.
27. M. Zhang, Y. Lu, J.-F. Chen, T.-K. Zhang, Y.-Y. Liu, Y. Yang, W.-T. Yao and S.-H. Yu, *Langmuir*, 2010, **26**, 12882-12889.
28. R. Wu, Y. Xu, R. Xu, Y. Huang and B. Zhang, *J. Mater. Chem. A*, 2015, DOI: 10.1039/C4TA05729E..
29. H.-L. Gao, L. Xu, F. Long, Z. Pan, Y.-X. Du, Y. Lu, J. Ge and S.-H. Yu, *Angew. Chem. Int. Ed.*, 2014, **53**, 4561-4566.
30. X. Fei, W. Li, Z. Shao, S. Seeger, D. Zhao and X. Chen, *J. Am. Chem. Soc.*, 2014, **136**, 15781-15786.
31. L. Zhang and X. W. Lou, *Chem. Eur. J.*, 2014, **20**, 5219-5223.

32. L. Zhang, H. B. Wu, Y. Yan, X. Wang and X. W. Lou, *Energy Environ. Sci.*, 2014, **7**, 3302-3306.
33. L. Yu, G. Q. Zhang, C. Z. Yuan and X. W. Lou, *Chem. Commun.*, 2013, **49**, 137-139.
34. Z. Xiong and X. S. Zhao, *J. Am. Chem. Soc.*, 2012, **134**, 5754-5757.
35. J. Yu, J. Low, W. Xiao, P. Zhou and M. Jaroniec, *J. Am. Chem. Soc.*, 2014, **136**, 8839-8842.
36. L. Q. Jing, W. Zhou, G. H. Tian and H. G. Fu, *Chem. Soc. Rev.*, 2013, **42**, 9509-9549.
37. Y. J. Chen, G. H. Tian, Z. Y. Reng, K. Pan, Y. H. Shi, J. Q. Wang, H. G. Fu, *ACS Appl. Mater. Int.* 2014, **6**, 13841-13849.
38. Y. Yu, G. Chen, Q. Wang and Y. Li, *Energy Environ. Sci.*, 2011, **4**, 3652-3660.
39. T. Bian, L. Shang, H. Yu, M. T. Perez, L.-Z. Wu, C.-H. Tung, Z. Nie, Z. Y. Tang and T. R. Zhang, *Adv. Mater.*, 2014, **26**, 5613-5618.
40. Y. Li, G. Duan, G. Liu and W. Cai, *Chem. Soc. Rev.*, 2013, **42**, 3614-3627.
41. M. Guerrero, S. Pane, B. J. Nelson, M. D. Baro, M. Roldan, J. Sort and E. Pellicer, *Nanoscale*, 2013, **5**, 12542-12550.
42. M. A. Zeeshan, R. Grisch, E. Pellicer, K. M. Sivaraman, K. E. Peyer, J. Sort, B. Özkale, M. S. Sakar, B. J. Nelson and S. Pané, *Small*, 2014, **10**, 1234-1234.
43. Q. Peng, Y. Dong and Y. Li, *Angew. Chem. Int. Ed.*, 2003, **42**, 3027-3030.
44. N. Pradhan, D. M. Battaglia, Y. Liu and X. Peng, *Nano Lett.*, 2006, **7**, 312-317.
45. N. Pradhan and X. Peng, *J. Am. Chem. Soc.*, 2007, **129**, 3339-3347.
46. K. Wang, J. Chen, W. Zhou, Y. Zhang, Y. Yan, J. Pern and A. Mascarenhas, *Adv. Mater.*, 2008, **20**, 3248-3253.
47. A. B. Panda, S. Acharya and S. Efrima, *Adv. Mater.*, 2005, **17**, 2471-2474.
48. S.-W. Kim, J. P. Zimmer, S. Ohnishi, J. B. Tracy, J. V. Frangioni and M. G. Bawendi, *J. Am. Chem. Soc.*, 2005, **127**, 10526-10532.
49. V. Šrot, A. Recnik, C. Scheu and B. Mirtic, *Microsc. Microanal.*, 2004, **10**, 316-317.
50. Q. Yu, L. Qi, K. Chen, R. K. Mishra, J. Li and A. M. Minor, *Nano Lett.*, 2012, **12**, 887-892.
51. L. Lu, Y. Shen, X. Chen, L. Qian and K. Lu, *Science*, 2004, **304**, 422-426.
52. S. Sun, D. Deng, C. Kong, X. Song and Z. Yang, *Dalton Trans.*, 2012, **41**, 3214-3222.
53. M. Liu, L. Wang, G. Lu, X. Yao and L. Guo, *Energy Environ. Sci.*, 2011, **4**, 1372-1378.
54. L. Ruan, E. Zhu, Y. Chen, Z. Lin, X. Huang, X. Duan and Y. Huang, *Angew. Chem. Int. Ed.*, 2013, **52**, 12577-12581.
55. S. Acharya, S. Sarkar and N. Pradhan, *Phys. Chem. Lett.*, 2012, **3**, 3812-3817.
56. Y. Zhang, Y. Tang, X. Liu, Z. Dong, H. H. Hng, Z. Chen, T. C. Sum and X. D. Chen, *Small*, 2013, **9**, 996-1002.
57. J. R. Ran, J. Zhang, J. Yu, M. Jaroniec and S. Z. Qiao, *Chem. Soc. Rev.*, 2014, **43**, 7787-7812.
58. J. Liu, G. K. Zhang, J. C. Yu and Y. D. Guo, *Dalton Trans.*, 2013, **42**, 5092-5099
59. Z. R. Shen, S. T. Sun, W. J. Wang, J. W. Liu, Z. F. Liu and J. C. Yu, *J. Mater. Chem. A*, 2015, DOI:10.1039/c4ta06871h.
60. L. Shang, T. Bian, B. Zhang, D. Zhang, L.-Z. Wu, C.-H. Tung, Y. D. Yin and T. R Zhang, *Angew. Chem. Int. Ed.*, 2014, **53**, 250-254.
61. V. R. Stamenkovic, B. Fowler, B. S. Mun, G. Wang, P. N. Ross, C. A. Lucas and N. M. Marković, *Science*, 2007, **315**, 493-497.
62. K. Yoon, Y. Yang, P. Lu, D. Wan, H.-C. Peng, K. Stamm Masias, P. T. Fanson, C. T. Campbell and Y. Xia, *Angew. Chem. Int. Ed.*, 2012, **51**, 9543-9546.
63. P. Xu, R. Yu, H. Ren, L. Zong, J. Chen and X. Xing, *Chem. Sci.*, 2014, **5**, 4221-4226.



 

**Supplementary Information**

# Converting 2D Inorganic-organic ZnSe-DETA Hybrid Nanosheets into 3D Hierarchical Nanosheet-based ZnSe Microspheres with Enhanced Visible-light-driven Photocatalytic Performances

Xuan Wu,‡[a] Rui Xu,‡[a] Rongjiao Zhu,*[a] Rui Wu[ab] and Bin Zhang*[a]

[a] *Department of Chemistry, School of Science, Tianjin University, and Collaborative Innovation Center of Chemical Science and Engineering (Tianjin), Tianjin, 300072, P. R. China. E-mail: bzhang@tju.edu.cn (B. Z.) zhurongjiao@tju.edu.cn (R. Z.)*

[b] *School of Chemical Engineering and Technology, Tianjin University, Tianjin, 300072, P. R. China.*

‡ *These authors contributed equally to this work.*

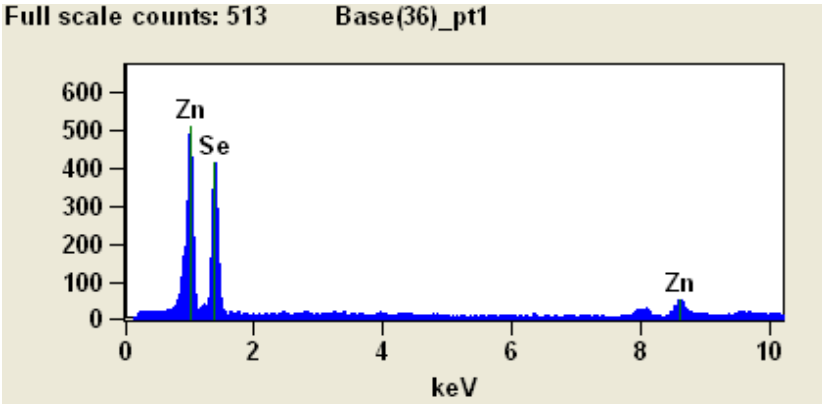


**Figure S1.** EDX spectra of the as-prepared hierarchical nanosheet-based ZnSe microspheres.

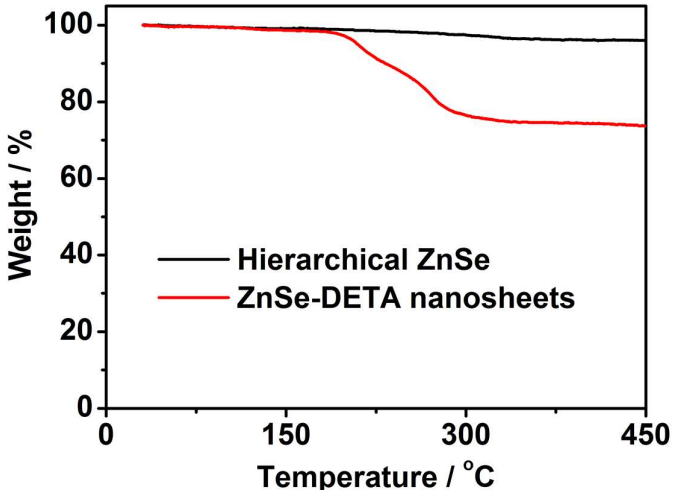


**Figure S2.** TGA curves of 3D hierarchical ZnSe products (black line) and ZnSe precursor (red line).

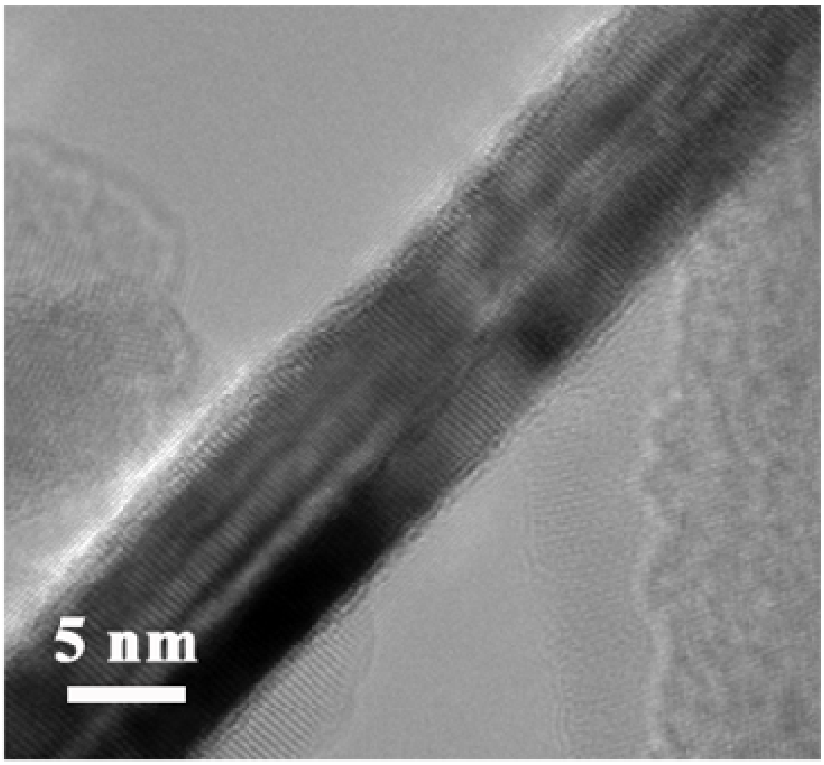


**Figure S3.** TEM image of a perpendicularly isolated ZnSe nanosheet that constructed the hierarchical nanostructures obtained at 150 °C.

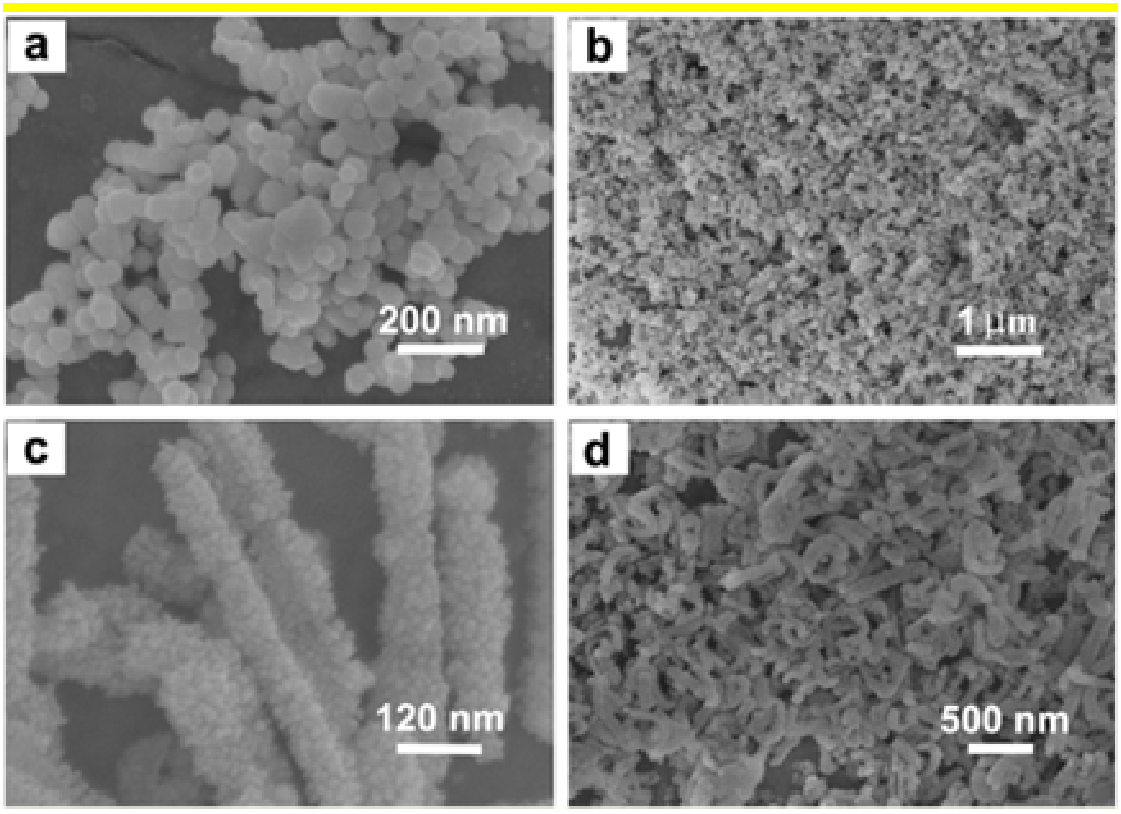


**Figure S4.** SEM images of the products obtained through the organic-component depleted reaction of the rinsed ZnSe-DETA hybrid nanosheets: ZnSe nanoparticles (a, b) obtained by removing the DETA and $N_2H_4{\cdot}H_2O$ in the reaction solution and nanoparticle arrayed ZnSe (c, d) obtained by introducing $N_2H_4{\cdot}H_2O$ (0.8 mL) in the absence of DETA in the reaction system.

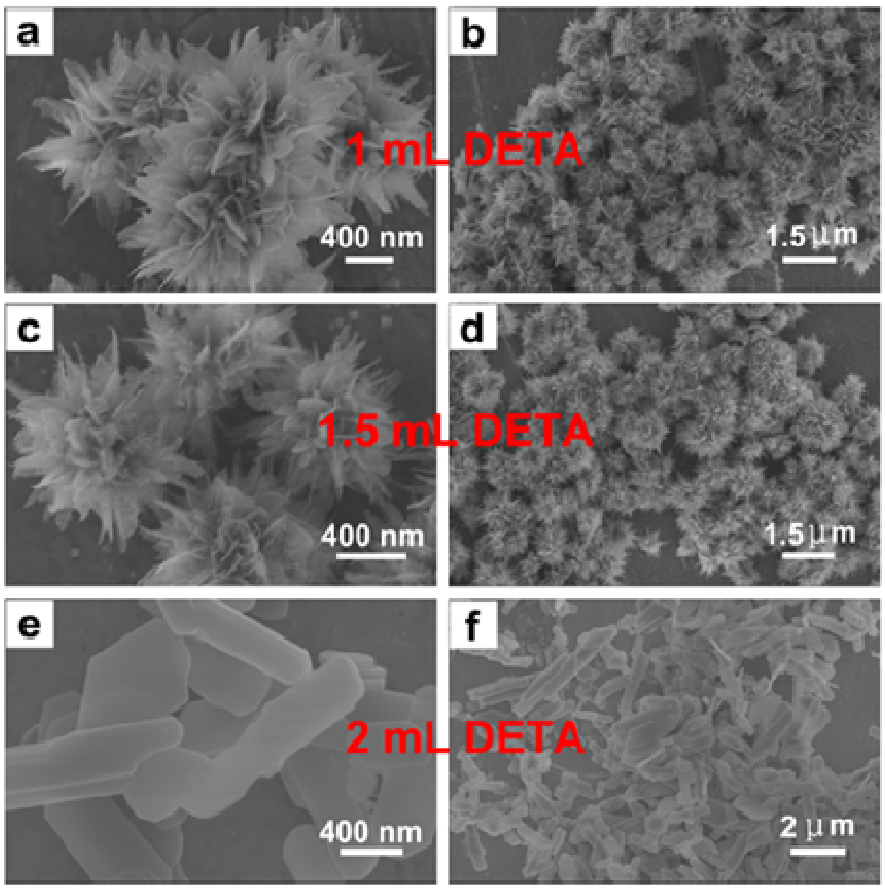


**Figure S5.** SEM images of the products obtained through the transformation reaction of the rinsed ZnSe-DETA sheets by introducing different amounts of DETA into the reaction systems: a, b): 1 mL DETA; c, d): 1.5 mL DETA; e, f): 2.0 mL DETA.

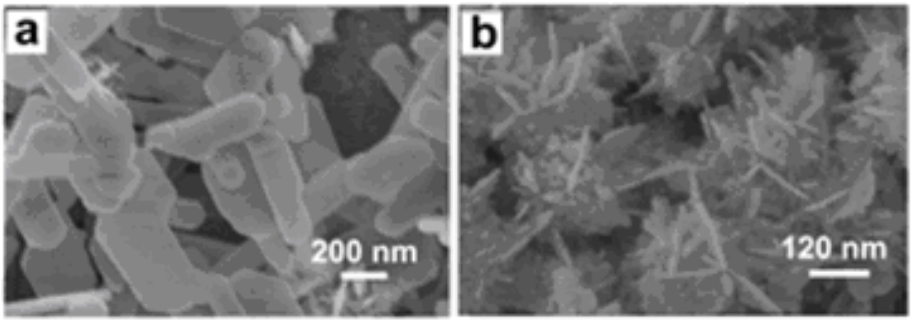


**Figure S6.** SEM images of the products obtained at different reaction temperatures: 140 °C (a) and 180 °C (b).

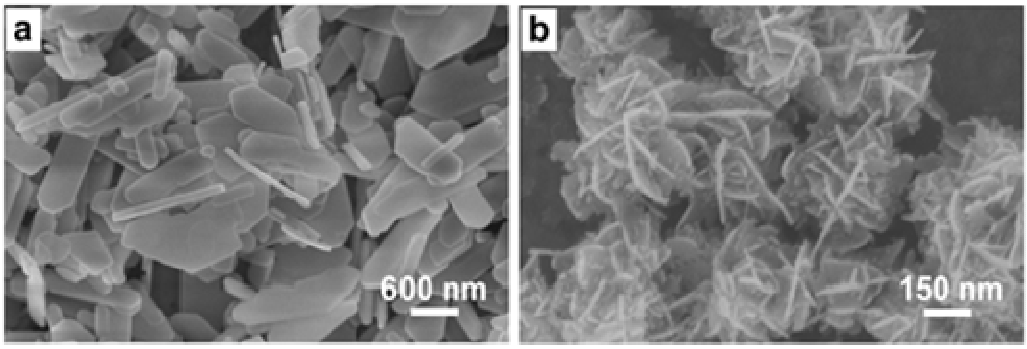


**Figure S7.** SEM images of the products prepared by the transformation reaction of inorganic-organic hybrid ZnSe-DETA nanosheets in EG at 150 ℃ (a) and 180 ℃ (b).

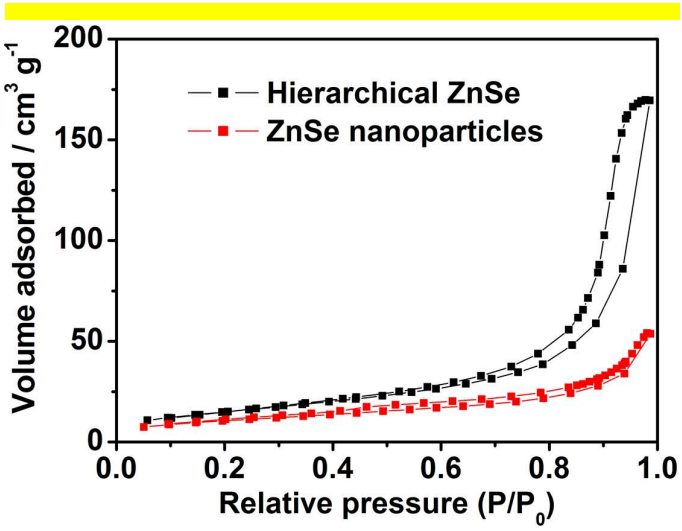


**Figure S8.** $N_2$ adsorption isotherm curves of hierarchical nanosheet-based ZnSe microspheres (black line) and ZnSe nanoparticles (red line).

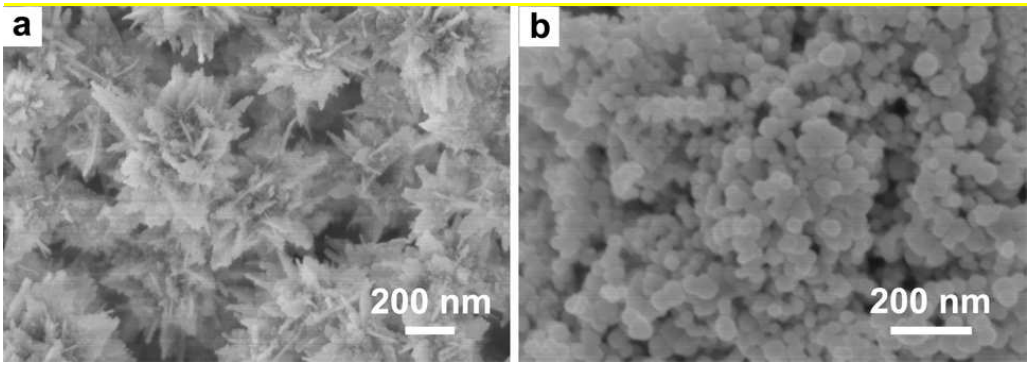


**Figure S9.** SEM images of the ZnSe flower (a) and the ZnSe particle (b) after the 12 h photocatalytic hydrogen evolution.

# A Table of Contents Entry

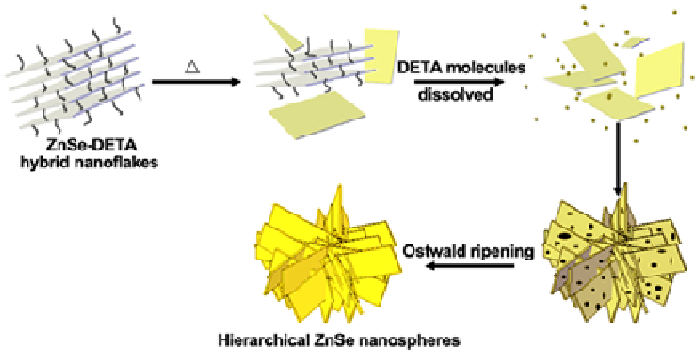


**3D hierarchical nanosheet-based ZnSe microspheres with improved photocatalytic performance were synthesized via of facile chemical conversion strategy of 2D inorganic-organic hybrid ZnSe-DETA nanosheets.**

Journal Name

RSCPublishing

ARTICLE

# Converting 2D Inorganic-organic ZnSe-DETA Hybrid Nanosheets into 3D Hierarchical Nanosheet-based ZnSe Microspheres with Enhanced Visible-light-driven Photocatalytic Performances

Cite this: DOI: 10.1039/x0xx00000x

Received 00th January 2012,
Accepted 00th January 2012

DOI: 10.1039/x0xx00000x

www.rsc.org/

Xuan Wu,[‡a] Rui Xu,[‡a] Rongjiao Zhu,[*a] Rui Wu[ab] and Bin Zhang[*a]

Engineering two-dimensional (2D) nanosheets into three-dimensional (3D) hierarchical structure is one of the great challenges in nano chemistry and material science. We report a facile and simple chemical conversion route to fabricate 3D hierarchical nanosheet-based ZnSe microspheres by using 2D inorganic-organic hybrid ZnSe-DETA (DETA=diethylenetriamine) nanosheets as the starting precursors. The conversion mechanism involves the controlled depletion of the organic-component (DETA) from the hybrid precursors and the subsequent self-assembly of the remnant inorganic-component (ZnSe). The transformation reaction of ZnSe-DETA nanosheets is mainly influenced by the concentration of DETA in the reaction solution. We demonstrated that this organic-component depletion method could be extended to the synthesis of other hierarchical structures of metal sulfides. Additionally, the obtained hierarchical nanosheet-based ZnSe microspheres exhibited outstanding performance in visible light photocatalytic degradation of the methyl orange and were highly active for photocatalytic $H_2$ production.

## 1. Introduction

Nanostructures with fascinating properties and novel applications in catalysis, gas sensing, photonics, energy storage and bionanotechnology have inspired great increasing efforts to design and control the morphology, structure, and composition of the nanocrystals to optimize the properties of materials.[1-12] Diverse advanced chemical transformation strategies, such as ion-exchange reaction, the Kirkendall effect and stabilizer-depleted approaches, have been developed to convert one starting material into another desired target material which cannot be easily prepared by other methods.[13-17] Recently, we have developed a facile ion-exchange and organic component stripping strategy of inorganic-organic hybrid nanowires or nanosheets to fabricate hierarchical porous $MoS_2$ nanotubes or $Cd_xZn_{1-x}Se$ hollow nanoframes.[18-19] And unary porous single-crystal-like semiconductor Te nanoplates could be generated from binary materials through an organic compound assistant depletion method.[20] In particular, stabilizer-depleted method, which based on the removal of the organic stabilizer and the spontaneous self-assembly of the individual inorganic building blocks, has emerged as a charming strategy for the synthesis of nanomaterials with tunable morphology and even more complex structures as well as unique properties.[21] At present, most of these researches were mainly focused on the transformation from nanoparticles to the nanowires by the action of the stabilizer. For example, Se and Te nanowires resulted from the interesting spontaneous reorganization of their binary semiconductor nanoparticles have been investigated in detail.[22, 23] This stabilizer-depleted method can also be utilized for the preparation of nanowires from noble metals.[24] Additionally, the *in situ* self-assembly of the nanoparticles via the partial removal of the organic stabilizer can also be used for the synthesis of some other shaped nanomaterials.[13, 25] Oil-phase synthesis of some crystalline nanoflowers via the limited ligand protection strategy has been previously studied by Peng group.[26] Yu and co-workers have reported that hybrid nanobelts can be transformed into inorganic nanotubes due to the release of the stabilizer in the selected organic solvents.[27] Despite of these progresses in stabilizer-depleted synthesis of nanomaterials, the production of three-dimensional (3D) hierarchical inorganic nanostructures via the depletion of the organic component from inorganic-organic hybrid nanosheets has not been adequately developed.[28]

Hierarchical structures composed of diverse nanocrystals have attracted worldwide attention owing to their unique properties and widespread potential applications in various

fields, which are different from and even surpass their primary structures.[4, 29-38] For instance, Lou and co-workers demonstrated that hierarchical nanostructures owned the fascinating performance in energy conversion and storage.[31-33] Currently, a wide range of strategies such as self-assembly of the primary building blocks or template-assisted fabrication, chemical vapor deposition, electron irradiation and bottom-up growth method have been developed to fabricate semiconductor nanocomposites with hierarchical nanostructures.[39-42] As one of the most well-known II–VI semiconductor materials, ZnSe, with a direct band gap of 2.67 eV and excellent optoelectronic properties, has been widely studied for the promising photovoltaic applications.[43-48] However, the development of a facile and universal approach to synthesize 3D hierarchical nanosheet-based ZnSe micromaterials on large scale for the photocatalytic application is still in its infancy.

Herein, we report a facile and effective way to prepare 3D hierarchical ZnSe microspheres via the depletion of organic component of unpurified inorganic–organic 2D ZnSe–DETA hybrid nanosheets. It has been shown that nanosheet-based ZnSe microspheres can be synthesized by tuning the concentration of DETA in the reaction solution. Moreover, this organic-component depletion method of hybrid nanosheets may be also suitable for fabricating hierarchical sphere-like nanostructures of other sulfides and selenides. The subsequent performance test shows that the as-prepared inorganic hierarchical ZnSe microspheres with the mixture of single-crystalline and twinning structure exhibit enhanced performance in the photocatalytic degradation of methyl orange (MO) and photocatalytic hydrogen production.

## 2. Experimental section

### 2.1. Chemicals

All chemicals are analytical grade and were used as received without further purification. Aqueous solutions were prepared using deionized water (DIW).

### 2.2. Synthesis of hybrid ZnSe-DETA and ZnS-DETA nanosheets.

Inorganic-organic hybrid nanosheets were prepared as our previously reported method.[17]

### 2.3. Synthesis of hierarchical nanosheet-based ZnSe microspheres.

For the synthesis of inorganic hierarchical nanosheet-based ZnSe microspheres, 0.3 mmol unpurified ZnSe-DETA nanosheets (about 3.4 mL) were dispersed into 16 mL DIW under vigorous stirring, then the mixture was transferred into 20 mL Teflon-lined stainless-steel autoclave and kept at 150 °C for 12 h, and cooled down naturally. The resultant yellow products were collected by centrifuging and washed with absolute ethanol and DIW for several times to remove any possible remained amine, and then dried under a vacuum at 40 ºC for 6 h for further use.

### 2.4. Synthesis of hierarchical nanosheet-based ZnS microspheres.

The procedure for the synthesis of inorganic ZnS 3D hierarchical microspheres is the same to that of ZnSe microspheres except that the ZnSe-DETA nanosheets were replaced by ZnS-DETA nanosheets.

### 2.5. Synthesis of ZnSe nanoparticles.

For the synthesis of ZnSe nanoparticles, ZnSe-DETA nanosheets were first rinsed to remove adsorbed $N_2H_4 \cdot H_2O$ and DETA, then about 0.3 mmol purified ZnSe-DETA nanosheets were dispersed into 16 mL DIW under vigorous stirring, the as-prepared dispersion was finally transferred into 20 mL Teflon-lined stainless-steel autoclave and kept at 150 °C for 12 h.

### 2.6. Characterization

The scanning electron microscopy (SEM) images were taken with a Hitachi S-4800 scanning electron microscope (SEM, 3 kV). Transmission electron microscopy (TEM), higher-magnification transmission electron microscopy (HRTEM) images were obtained with JEOL-2100F system. Specimens for TEM and HRTEM measurements were prepared via dropcasting a droplet of ethanol suspension onto a copper grid, coated with a thin layer of amorphous carbon film, and allowed to dry in air. The X-ray diffraction patterns (XRD) of the products were recorded with Bruker D8 Focus Diffraction System using a Cu Kα source (λ= 0.154178 nm). FTIR spectra were recorded on a MAGNA-IR 750 (Nicolet Instrument Co) FTIR spectrometer. UV-vis diffuse reflectance spectra (UV-vis DRS) were recorded on a Lambda 750S UV–vis-NIR spectrometer (Perkin-Elmer) equipped with an integrating sphere. The UV-vis DRS of solid samples were collected in 200–800 nm against $BaSO_4$ reflectance standard. The surface area was determined by nitrogen physisorption using Quadrasorb SII Quantachrome Instrumen and calculated using the Brunauer-Emmett-Teller (BET) method. Thermogravimetric analysis (TGA) was measured by NETZSCH STA 409 analyzer with a ramp rate of 10 ºC $min^{-1}$ from room temperature to 450 °C at the $N_2$ atmosphere.

### 2.7. Photocatalytic degradation of methyl orange

The photocatalytic activities of 3D hierarchical ZnSe microspheres for the degradation of methyl orange (MO) were carried out under visible-light irradiation. For each test of MO degradation, 30 mg catalyst power was dispersed into 100 mL of $5\times10^{-5}$ M MO solution. A 300 W Xe lamp equipped with a cutoff filter (λ > 420 nm) was used as the optical system. The suspension solution was kept stirring at room temperature for 10 h in the dark to ensure the absorption equilibrium of the water, MO and the catalyst. The distance between the Xe lamp and the reaction solution was about 18 cm. Then the mixture solution was exposed to visible-light irradiation under constantly stirring. A water bath connected to the flowing water was used to keep the whole reaction solution maintain at room



 

temperature. The concentration of MO was analyzed by UV-vis spectrophotometer.

### 2.8. Photocatalytic hydrogen evolution

For the photocatalytic hydrogen production, a 100 mL top-irradiation Pyrex cell reactor and a 300 W Xe lamp equipped with a cutoff filter ($\lambda > 420$ nm) were employed. The Pyrex flask was cooled by the flowing water to keep the tests at room temperature. Before exposing to the visible light irradiation, approximately 30 mg catalyst power was dispersed into 50 mL aqueous solution containing 0.5 M $Na_2S$ and 0.5 M $Na_2SO_3$ as the sacrificial reagents and stabilizer, and then the mixture was sonicated for about 5 minutes to prepare homogenous dispersion. The composition of products mixture was analyzed with an on-line Agilent 7890A gas chromatography equipped with a TCD detector.

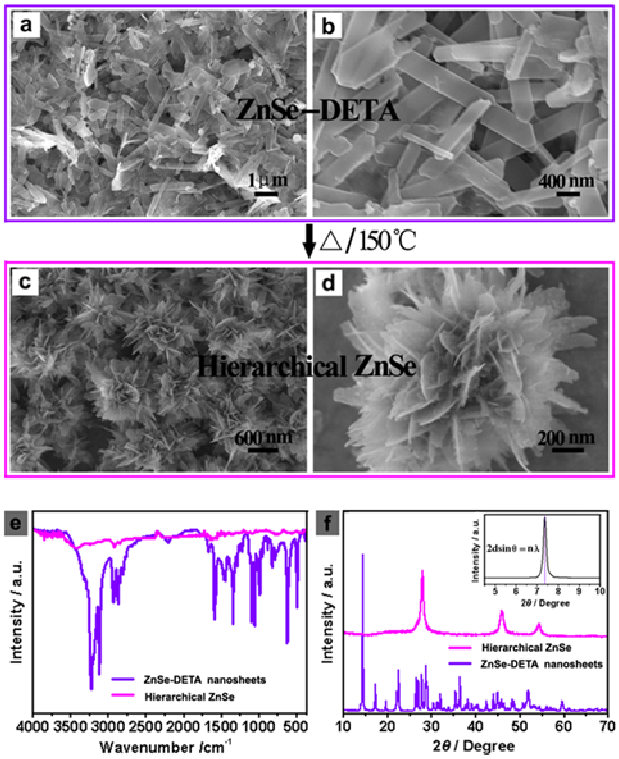


**Figure 1.** (a, b) SEM images of the ZnSe-DETA nanosheets. (c, d) Typical SEM images of the as prepared 3D hierarchical ZnSe microspheres obtained by the hydrothermal transformation of the ZnSe-DETA hybrid nanosheets through the organic-component depletion method. (e) FTIR spectra of the ZnSe-DETA hybrid nanosheets (purple line) and inorganic ZnSe hierarchical microstructures (magenta line). (f) XRD patterns of ZnSe-DETA nanosheets (purple, lower trace), ZnSe hierarchical microspheres (magenta, upper trace) and low-angle XRD pattern of ZnSe-DETA (inset).

## 3. Results and discussion

The ZnSe–DETA nanosheets were prepared using a modified amine-assisted solvothermal method and then used as starting materials to obtain inorganic hierarchical nanosheet-based ZnSe microspheres under the hydrothermal condition. The size and morphology of the hybrid ZnSe–DETA nanosheets were first examined by SEM. Low-magnification SEM image in Figure 1a shows that the ZnSe–DETA nanosheets could be synthesized successfully. High-magnification SEM image demonstrates that these nanosheets possess a thickness of about 80 nm (Figure 1b). FTIR spectrum (Figure 1e) and XRD pattern (Figure 1f) further identify the obtained samples as inorganic-organic hybrid ZnSe-DETA nanosheets. The small angle XRD pattern (the inset of Figure 1f) indicates that these hybrid precursors own the layered structure with an interlayer spacing of about 1.2 nm (calculated by Prague formula). The unpurified ZnSe–DETA nanosheets were then used as the starting materials and hydrothermally treated at 150 °C for 12 h to obtain the products. Representative SEM image shows that the products are uniform spherical structure with diameters of 1 μm (Figure 1c). High-magnification SEM image (Figure 1d) demonstrates that the as-prepared ZnSe microspheres are hierarchical architectures of irregular nanosheets. Energy-dispersive X-ray (EDX) spectrum (Figure S1, Supporting Information) displays the samples are composed of pure Zn and Se. The ratio of Zn to Se is ca. 1. FTIR spectra (Figure 1e) suggest the transformation of hybrid ZnSe-DETA precursors to the inorganic hierarchical microstructures. In the typical XRD pattern of the as-converted hierarchical nanosheet-based microspheres (Figure 1f), all the diffraction peaks can be indexed to the wurtzite phase of ZnSe (JCPDS 15-0105), implying that the as-obtained hierarchical microspheres are ZnSe with high purity. Organic contents in the precursors and in the products are analyzed using TGA (Figure S2, Supporting Information). The decomposition of ZnSe precursor begins at 150 °C and ends at about 350 °C, with total weight loss of 25.3%, confirming the molecular formula of inorganic-organic hybrids as ZnSe-$(DETA)_{0.5}$. As for the 3D hierarchical ZnSe products, the organic content in the products is negligible because there's no obvious weight loss in this range.

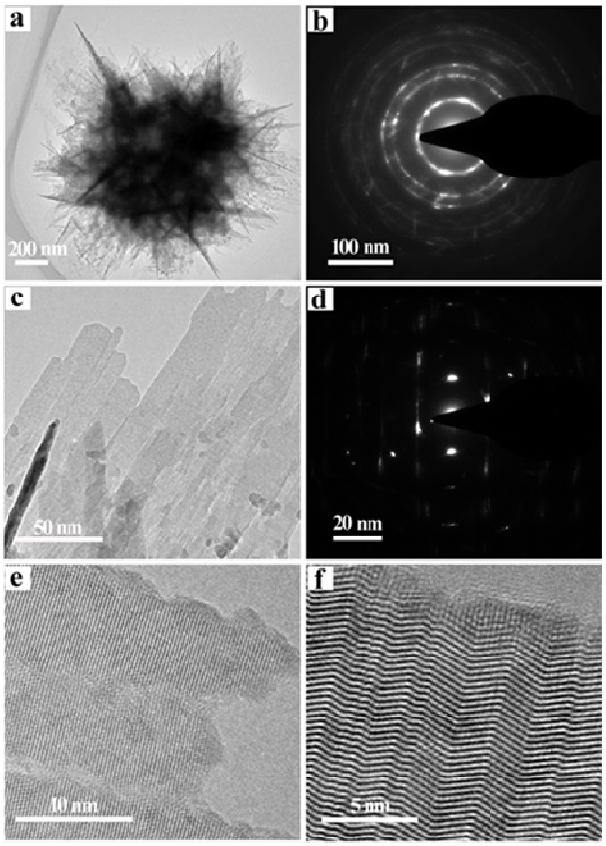


**Figure 2.** (a) TEM image of the ZnSe hierarchical microstructure; (b) corresponding SAED pattern of an individual ZnSe microsphere. (c) TEM image of the individual ZnSe nanosheet, (d) the SAED pattern of the nanosheets which compose the hierarchical structures. (e, f) HRTEM of the ZnSe nanosheets.

The morphology and structure of the hierarchical nanosheet-based ZnSe microspheres were further studied by transmission electron microscopy (TEM), selected area electron diffraction (SAED) and high-resolution TEM (HRTEM). Typical TEM image of the inorganic ZnSe microspheres presented in Figure 2a indicates that these hierarchical structures are composed of irregular nanosheets. The associated SAED pattern of the individual microsphere displayed in Figure 2b confirms that these hierarchical ZnSe structures are polycrystalline. The representative TEM image of the fringe of an individual ZnSe nanosheet (Figure S3, Supporting Information) indicates that the thickness of irregular nanosheets in hierarchical nanosheet-based microspheres is about 5-8 nm. TEM image displayed in Figure 2c further shows that these microspheres are hierarchical architecture of nanosheets. The associated SAED pattern of one main sheet (Figure 2d) and their HRTEM images (Figure 2e, f) show that there exists the mixture of single-crystal-like and twinning superlattice phases in the ZnSe hierarchical microspheres. The appearance of twinning crystal may be attributed to the changes in the selenium fugacity, and such twinning structure may exert a noticeable influence on the optical, electronic and mechanical properties of the as-prepared ZnSe hierarchical microspheres.[49-54] These results testify that inorganic-organic hybrid ZnSe-DETA nanosheets can be successfully transformed into inorganic hierarchical nanosheet-based ZnSe microspheres with the mixed single-crystalline and twinning structure.

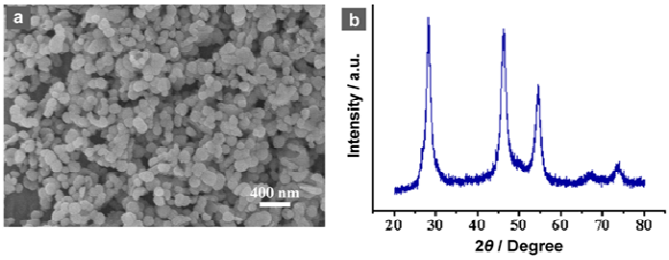


**Figure 3.** SEM image (a) and XRD pattern (b) of the ZnSe nanoparticals.

It should be pointed out that the unpurified ZnSe–DETA nanosheets obtained from the amine-assisted solvothermal method contains the superfluous $N_2H_4 \cdot H_2O$ and DETA. To further explore the formation process, the roles of the $N_2H_4 \cdot H_2O$ and DETA on the structure transformation were studied. When ZnSe-DETA samples were rinsed to completely remove adsorbed $N_2H_4 \cdot H_2O$ and DETA, and were then used as the starting precursors with other conditions unchanged, the products were irregular inorganic wurtzite ZnSe nanoparticles with a diameter of 40-100 nm (Figure 3 and Figure S4a, b, Supporting Information). When rinsed ZnSe-DETA samples were mixed with an appropriate amount of $N_2H_4 \cdot H_2O$ in the absence of DETA and reacted in the same hydrothermal condition, aggregation of nanoparticles was obtained (Figure S4c, d, Supporting Information). These results suggest that DETA plays an important role in the transformation of ZnSe-DETA hybrid nanosheets into inorganic nanosheet-based ZnSe hierarchical structures. We also found that the concentration of DETA in the solution exerted a remarkable influence on the transformation of the hybrid nanosheets. When an appropriate amount of DETA was introduced into the hydrothermal reaction system, ZnSe hierarchical microstructures can also be generated (Figure S5a-d, Supporting Information). However, once excessive DETA ($V_{DETA} \geq 2$ mL) was added, the high concentration of DETA in the solution will hamper the dissolution of DETA from the hybrid nanosheets into the reaction system, and then the transformation from ZnSe-DETA hybrid nanosheets to the hierarchical ZnSe microstructures will be prevented (Figure S5e-f, Supporting Information). Therefore, we can speculate that the concentration of the DETA in the hydrothermal solution plays a key role in the transformation reaction.

We have also found that the reaction temperature and the solvent play important roles in the conversion of inorganic-organic hybrid ZnSe-DETA nanosheets. When DIW was used as the solvent for the transformation reaction at 180 °C, the products generated from the reaction were hierarchical ZnSe microspheres with a size of about 1 μm (Figure S6b, Supporting Information). But, once the reaction temperature is lower than 150 °C, the reaction would be difficult to initiate (Figure S6a, Supporting Information). On the other hand, 3D hierarchical



 

ZnSe microstructures can also be generated when ethylene glycol (EG) was used as the reaction medium, while the transformation process may need to react at higher temperature (more than 180 °C), and the size of obtained structures is around 300 nm (Figure S7, Supporting Information). The solvent has a noticeable influence on the transformation products, which may be associated with the solvability of DETA in different solvents. When the transformation reaction was performed in EG, the reaction needs higher temperature probably due to the slow release of the DETA in the EG solution.

To gain insight into the transformation mechanism of the reaction, the morphology and phase transformation processes were investigated by performing the time-dependent experiments SEM and XRD were used to characterize the intermediates collected at different stages of the reaction. The local structural variations of ZnSe could also know from the SEM images (inset in Figure 4). When the reaction proceeded for 1h, a few wall-like embryonic products were obtained (Figure 4a), which may be generated due to the partial release of the DETA molecules between the layers of the ZnSe-DETA hybrid precursors. The corresponding XRD pattern displayed in Figure 4g revealed that these samples were mainly ZnSe-DETA nanosheets. After the reaction proceeding for 2 h, the thickness of precursor nanosheets decreased while the amount of the embryonic products composed of thin walls increased and some walls were intertwined together to generate the early flower-like products (Figure 4b). If the reaction time was prolonged to 3 h, light yellow product composed of ZnSe flower-like rudiments and semi-finished nanosheets were obtained. The latter can serve as the subsequent resources for the following growth of the ZnSe microspheres (Figure 4c). When the reaction time was increased to 4 h, the individual nanosheets almost disappeared, and the samples mostly became hierarchical ZnSe nanostructures (Figure 4d). The prolonged exchange reaction and the slow dissolution of DETA in water made the middle area of the sheets break into small particles and the edges became bigger and rougher, and a mass of small nanoparticles generated along with the reaction were found in the reaction solution (inset of Figure 4d). After 6 h, the dispersed ZnSe nanoparticles in the solution disappeared and were found to adsorb on the surfaces of the 3D hierarchical ZnSe microspheres, as shown in Figure 4e. As confirmed by XRD patterns in Figure 4g, along with the reaction time, the amount of DETA in the intermediates decreased and the intermediates transformed gradually into inorganic ZnSe hierarchical structures of wurtzite phase. When the reaction is prolonged to 10 h, the small nanoparticles disappeared gradually and recrystallized onto the pre-generated platelets. So the surfaces of the microspheres became more smooth and perfectly transformed 3D hierarchical ZnSe structures were obtained (Figure 4f). Moreover, the phase transformation characterized by XRD pattern in Figure 4g revealed that the signal of the organic component was disappeared and pure wurtzite ZnSe phase was produced.

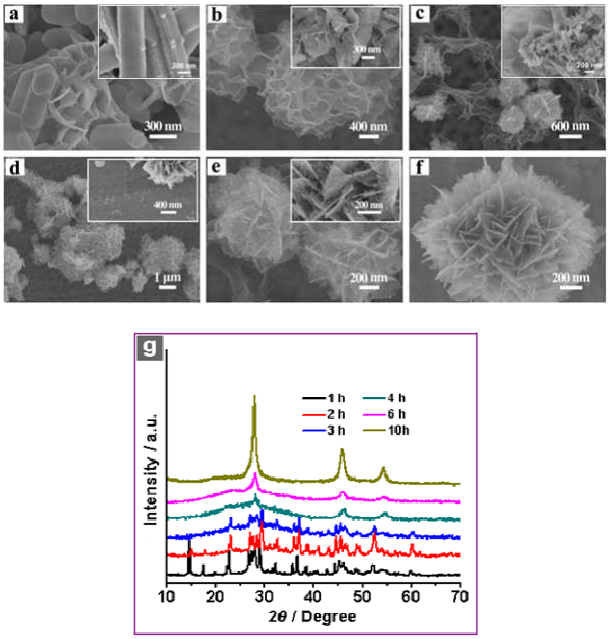


**Figure 4.** SEM images (a-f) and XRD patterns (g) of the intermediates collected after the transformation reaction proceeded for different times: a) 1 h, b) 2 h, c) 3 h, d) 4 h, e) 6 h, f) 10 h.

Organic amine molecules have been reported to play a key role in the fabrication of 2D metal sulfides.[55] Herein, on the base of the above-mentioned results, we propose a DETA-induced nucleation and self-assemble mechanism with following Ostwald ripening process for the chemical conversion of inorganic-organic hybrid ZnSe-DETA nanosheets into inorganic hierarchical nanosheet-based ZnSe microspheres. Firstly, the DETA molecules dissolve gradually from the hybrid precursors into the reaction solution at elevated temperature. Meanwhile, the residual ZnSe components turn into sheet-like embryonic structures via a dissolution-recrystallization process due to the induced role of DETA.[28, 55] Upon prolonging the reaction time, the as-generated sheet-like embryonic structures intertwined together to generate the early flower-like product through a self-assembly process. Finally, with the elongation of reaction time, thermodynamically stable hierarchical nanosheet-based ZnSe microspheres are obtained by the Ostwald ripening growth process (Scheme 1). Note that an additional systematic study is necessary to fully explore fundamental issues of size- and shape-dependent conversion activity for this strategy.

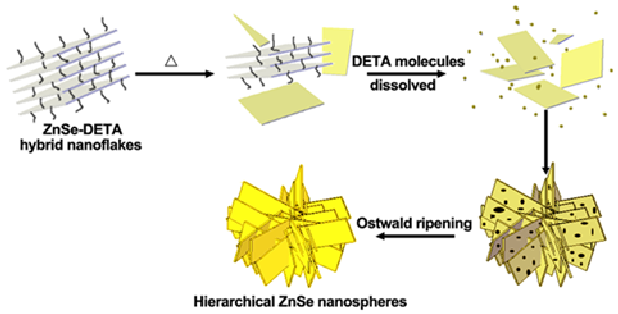


**Scheme 1.** Scheme illustrating the synthesis of inorganic hierarchical ZnSe microspheres through the organic-component depletion method of the unpurified inorganic-organic ZnSe-DETA hybrid nanosheets at 150 ºC.

Given these insights into the reaction that converts inorganic-organic ZnSe-DETA nanosheets to inorganic hierarchical nanosheet-based ZnSe microspheres and consideration of the chemical factors involved in the process, the conversion of other hybrid precursors to inorganic hierarchical structures may be expected. For instance, when unpurified inorganic-organic ZnS–DETA nanosheets were used as the starting materials for the transformation reaction in the hydrothermal solution at 150 °C, inorganic 3D hierarchical ZnS microspheres could also be generated (Figure 5). These results suggested this organic-component depletion triggered transformation reaction method presented herein might be expanded to the synthesis of microsphere-like structures of other metal sulfides and selenides.

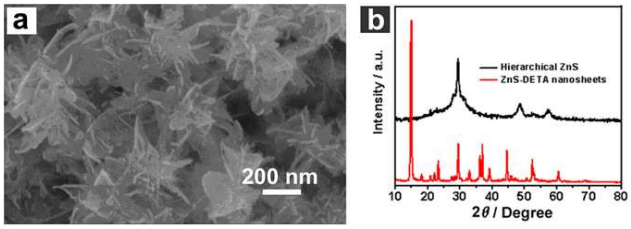


**Figure 5.** a) Typical SEM image of 3D hierarchical ZnS microspheres. b) XRD patterns of ZnS-DETA nanosheets (red line) and inorganic 3D hierarchical ZnS microspheres (black line).

Recently, semiconductor nano- and micron-materials with controlled morphologies and structures have been found to exhibit fascinating photocatalytic activities.[36, 56-60] Despite the advances in the synthesis of ZnSe nano- and micron-structures, the development of ZnSe nanomaterials with unique structures and improved catalytic activities under visible-light irradiation is still rarely reported. Herein, the photocatalytic dye degradation and photocatalytic hydrogen production of hierarchical ZnSe were measured for comparative studies with ZnSe nanoparticles. The photocatalytic activities of ZnSe for the degradation of methyl orange (MO) were carried out under visible-light irradiation ($\lambda > 420$ nm), and in each test, 30 mg catalyst power was utilized for the degradation of 100 mL MO ($5\times10^{-5}$ M) solution. The characteristic absorption peak of MO at 464 nm was measured to deliver the photocatalytic results. Figure 6a, b demonstrate the UV-vis absorption spectral changes of MO solution after the treatment of ZnSe catalysts along with the photocatalytic reaction hours, respectively. The diffuse reflectance UV-vis spectra of ZnSe nanoparticles and hierarchical fractal ZnSe nanospheres are presented in Figure 6c, indicating that the as-prepared hierarchical ZnSe possess improved photon capture ability compared to the ZnSe nanoparticles. The absorption profile of the hierarchical fractal ZnSe microspheres differs from the conventional ZnSe nanoparticles, which may arise from the morphology difference from 0D to 3D structure and the multiple scatter in the 3D hierarchical ZnSe microstructures. Figure 6d shows the degradation curves of MO in water under visible light irradiation in the presence of ZnSe catalysts, which clearly show that the degradation of MO is up to 97.1% after treatment by the hierarchical nanosheet-based ZnSe catalyst for 4h, while for the ZnSe nanoparticles it is only 39.6%.

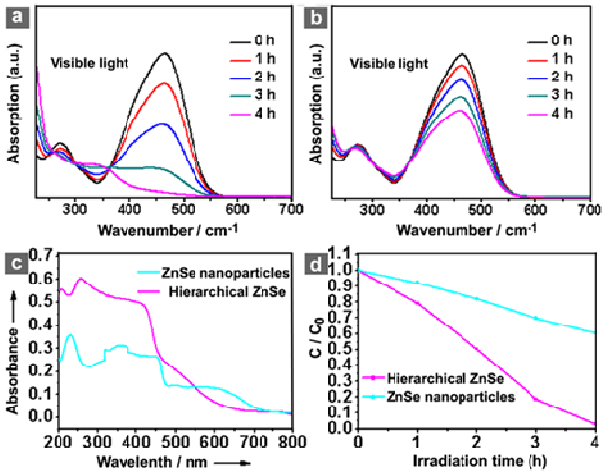


**Figure 6.** UV-visible absorption spectra for MO solutions under visible light in the presence of hierarchical fractal ZnSe (a) and ZnSe nanoparticles (b); (c) diffuse reflectance UV-vis spectra of ZnSe nanoparticles and 3D hierarchical ZnSe microspheres; (d) photobleaching curves of MO under visible light over ZnSe nanoparticles and 3D hierarchical ZnSe microstructures.

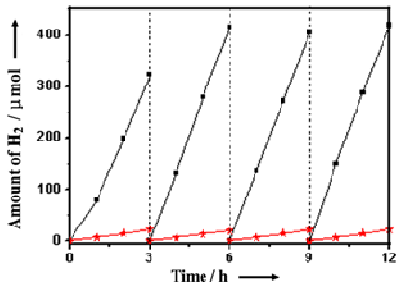


**Figure 7.** Time courses of $H_2$ evolution under the irradiation of visible-light of the as-prepared hierarchical nanosheet-based ZnSe microspheres (black, ■) and ZnSe nanoparticles (red, ★).

Furthermore, we have found that the as-prepared hierarchical nanosheet-based ZnSe microspheres exhibit enhanced catalytic performance for the photocatalytic hydrogen evolution under the irradiation of visible light. The surface area of ZnSe microspheres and ZnSe nanoparticles is characterized

using the BET method. As shown in Figure S8, hierarchical nanosheet-based ZnSe microspheres display the surface area of 55.163 $m^2 g^{-1}$, which is larger than that of ZnSe nanoparticles (37.563 $m^2 g^{-1}$). Figure 7 displays the reaction time courses for $H_2$ evolution under visible light over 3D hierarchical ZnSe microspheres and ZnSe nanoparticles. As shown in Figure 7, the photocatalytic reaction on hierarchical ZnSe microstructures exhibits a stable $H_2$-release rate of approximately 135 μmol $h^{-1}$ per 0.3 g of catalyst, which is about 18 times higher than that of ZnSe nanoparticles. The morphology stability of hierarchical ZnSe microstructures and ZnSe nanoparticles after the photocatalytic hydrogen evolution is identified by the SEM images (Figure S9, Supporting Information), which indicate their good durability. These results suggest that the as-prepared hierarchical ZnSe microspheres exhibit enhanced photocatalytic performance than ZnSe nanoparticles. This improved photocatalytic performance may be associated with the twinning structure of the ZnSe hierarchical nanosheets, which has enhanced the optical transitions to improve the photocatalytic performance.[53, 54] Additionally, the 3D hierarchical ZnSe microstructures lead to more active sites and higher stability of the catalysts.[61-63]

## 4. Conclusions

In summary, we have demonstrated a convenient organic-component depletion approach for the synthesis of inorganic hierarchical nanosheet-based ZnSe microspheres by utilizing the unpurified hybrid ZnSe-DETA nanosheets as the raw materials and treating them in the hydrothermal solution. The time-dependent morphology and phase conversion processes revealed that the transformation mechanism involving the slow dissolution of DETA, the following DETA-induced self-assembly process and the final Ostwald ripening growth. We also showed that this organic-component depletion method of inorganic-organic hybrid microstructures could be extended to the synthesis of other 3D hierarchical metal sulfides. In addition, the as-prepared hierarchical nanosheet-based ZnSe microspheres showed enhanced performances in visible light photocatalytic activities for both dye degradation and $H_2$ production.

## Acknowledgements

This work was financially supported by the National Natural Science Foundation of China (21422104 and 21373149) and the Innovation Foundation of Tianjin University.

## Notes and references

[a] *Department of Chemistry, School of Science, Tianjin University, and Collaborative Innovation Center of Chemical Science and Engineering (Tianjin), Tianjin, 300072, P. R. China. Fax&Tel: +86-22 27403475; E-mail: bzhang@tju.edu.cn (B. Z.) zhurongjiao@tju.edu.cn (R. Z.)*

[b] *School of Chemical Engineering and Technology, Tianjin University, Tianjin, 300072, P. R. China.*

† Electronic Supplementary Information (ESI) available: supplementary Figures: Figure S1–9. See DOI: 10.1039/b000000x/

‡ These authors contributed equally to this work.

1. M. A. Dobrovolskaia and S. E. McNeil, *Nature Nanotech.*, 2007, **2**, 469-478.
2. C.-H. Cui, H.-H. Li, J.-W. Yu, M.-R. Gao and S.-H. Yu, *Angew. Chem. Int. Ed.*, 2010, **49**, 9149-9152.
3. K. Zhou and Y. Li, *Angew. Chem. Int. Ed.*, 2012, **51**, 602-613.
4. S. Deng, V. Tjoa, H. M. Fan, H. R. Tan, D. C. Sayle, M. Olivo, S. Mhaisalkar, J. Wei and C. H. Sow, *J. Am. Chem. Soc.*, 2012, **134**, 4905-4917.
5. H. Zhang and H. Cui, *Nanoscale*, 2014, **6**, 2563-2566.
6. Y. Liu and Z. Tang, *Adv. Mater.*, 2013, **25**, 5819-5825.
7. Y. Zhu, C. Cao, S. Tao, W. Chu, Z. Wu and Y. Li, *Sci. Rep.*, 2014, **4**.
8. J. W. Hong, S.-U. Lee, Y. W. Lee and S. W. Han, *J. Am. Chem. Soc.*, 2012, **134**, 4565-4568.
9. S. Sun and Z. Yang, *Chem. Commun.*, 2014, **50**, 7403-7415.
10. M. Chen, B. Wu, J. Yang and N. Zheng, *Adv. Mater.*, 2012, **24**, 862-879.
11. Y. Wang, Y. Bai, X. Li, Y. Feng and H. Zhang, *Chem. Eur. J.*, 2013, **19**, 3340-3347.
12. Y. Mai, F. Zhang and X. Feng, *Nanoscale*, 2014, **6**, 106-121.
13. Z. Tang, Y. Wang, S. Shanbhag, M. Giersig and N. A. Kotov, *J. Am. Chem. Soc.*, 2006, **128**, 6730-6736.
14. D. H. Son, S. M. Hughes, Y. Yin and A. P. Alivisatos, *Science*, 2004, **306**, 1009-1012.
15. Y. Yin, R. M. Rioux, C. K. Erdonmez, S. Hughes, G. A. Somorjai and A. P. Alivisatos, *Science*, 2004, **304**, 711-714.
16. Y. Yu, X. Yin, A. Kvit and X. Wang, *Nano Lett.*, 2014, **14**, 2528-2535.
17. Y. Yu, J. Zhang, X. Wu, W. Zhao and B. Zhang, *Angew. Chem. Int. Ed.*, 2012, **51**, 897-900.
18. S. Zhuo, Y. Xu, W. Zhao, J. Zhang and B. Zhang, *Angew. Chem. Int. Ed.*, 2013, **52**, 8602-8606.
19. X. Wu, Y. Yu, Y. Liu, Y. Xu, C. Liu and B. Zhang, *Angew. Chem. Int. Ed.*, 2012, **51**, 3211-3215.
20. H. Zhang, H. Wang, Y. Xu, S. Zhuo, Y. Yu and B. Zhang, *Angew. Chem. Int. Ed.*, 2012, **51**, 1459-1463.
21. Z. Tang, Y. Wang, S. Shanbhag and N. A. Kotov, *J. Am. Chem. Soc.*, 2006, **128**, 7036-7042.
22. Z. Tang, N. A. Kotov and M. Giersig, *Science*, 2002, **297**, 237-240.
23. Z. Tang, Y. Wang, K. Sun and N. A. Kotov, *Adv. Mater.*, 2005, **17**, 358-363.
24. Y. Sun, B. Mayers, T. Herricks and Y. Xia, *Nano Lett.*, 2003, **3**, 955-960.
25. Z. Tang, P. Podsiadlo, B. S. Shim, J. Lee and N. A. Kotov, *Adv. Funct. Mater.*, 2008, **18**, 3801-3808.
26. A. Narayanaswamy, H. Xu, N. Pradhan and X. Peng, *Angew. Chem. Int. Ed.*, 2006, **45**, 5361-5364.
27. M. Zhang, Y. Lu, J.-F. Chen, T.-K. Zhang, Y.-Y. Liu, Y. Yang, W.-T. Yao and S.-H. Yu, *Langmuir*, 2010, **26**, 12882-12889.
28. R. Wu, Y. Xu, R. Xu, Y. Huang and B. Zhang, *J. Mater. Chem. A*, 2015, DOI: 10.1039/C4TA05729E..
29. H.-L. Gao, L. Xu, F. Long, Z. Pan, Y.-X. Du, Y. Lu, J. Ge and S.-H. Yu, *Angew. Chem. Int. Ed.*, 2014, **53**, 4561-4566.
30. X. Fei, W. Li, Z. Shao, S. Seeger, D. Zhao and X. Chen, *J. Am. Chem. Soc.*, 2014, **136**, 15781-15786.
31. L. Zhang and X. W. Lou, *Chem. Eur. J.*, 2014, **20**, 5219-5223.

32. L. Zhang, H. B. Wu, Y. Yan, X. Wang and X. W. Lou, *Energy Environ. Sci.*, 2014, **7**, 3302-3306.
33. L. Yu, G. Q. Zhang, C. Z. Yuan and X. W. Lou, *Chem. Commun.*, 2013, **49**, 137-139.
34. Z. Xiong and X. S. Zhao, *J. Am. Chem. Soc.*, 2012, **134**, 5754-5757.
35. J. Yu, J. Low, W. Xiao, P. Zhou and M. Jaroniec, *J. Am. Chem. Soc.*, 2014, **136**, 8839-8842.
36. L. Q. Jing, W. Zhou, G. H. Tian and H. G. Fu, *Chem. Soc. Rev.*, 2013, **42**, 9509-9549.
37. Y. J. Chen, G. H. Tian, Z. Y. Reng, K. Pan, Y. H. Shi, J. Q. Wang, H. G. Fu, *ACS Appl. Mater. Int.* 2014, **6**, 13841-13849.
38. Y. Yu, G. Chen, Q. Wang and Y. Li, *Energy Environ. Sci.*, 2011, **4**, 3652-3660.
39. T. Bian, L. Shang, H. Yu, M. T. Perez, L.-Z. Wu, C.-H. Tung, Z. Nie, Z. Y. Tang and T. R. Zhang, *Adv. Mater.*, 2014, **26**, 5613-5618.
40. Y. Li, G. Duan, G. Liu and W. Cai, *Chem. Soc. Rev.*, 2013, **42**, 3614-3627.
41. M. Guerrero, S. Pane, B. J. Nelson, M. D. Baro, M. Roldan, J. Sort and E. Pellicer, *Nanoscale*, 2013, **5**, 12542-12550.
42. M. A. Zeeshan, R. Grisch, E. Pellicer, K. M. Sivaraman, K. E. Peyer, J. Sort, B. Özkale, M. S. Sakar, B. J. Nelson and S. Pané, *Small*, 2014, **10**, 1234-1234.
43. Q. Peng, Y. Dong and Y. Li, *Angew. Chem. Int. Ed.*, 2003, **42**, 3027-3030.
44. N. Pradhan, D. M. Battaglia, Y. Liu and X. Peng, *Nano Lett.*, 2006, **7**, 312-317.
45. N. Pradhan and X. Peng, *J. Am. Chem. Soc.*, 2007, **129**, 3339-3347.
46. K. Wang, J. Chen, W. Zhou, Y. Zhang, Y. Yan, J. Pern and A. Mascarenhas, *Adv. Mater.*, 2008, **20**, 3248-3253.
47. A. B. Panda, S. Acharya and S. Efrima, *Adv. Mater.*, 2005, **17**, 2471-2474.
48. S.-W. Kim, J. P. Zimmer, S. Ohnishi, J. B. Tracy, J. V. Frangioni and M. G. Bawendi, *J. Am. Chem. Soc.*, 2005, **127**, 10526-10532.
49. V. Šrot, A. Recnik, C. Scheu and B. Mirtic, *Microsc. Microanal.*, 2004, **10**, 316-317.
50. Q. Yu, L. Qi, K. Chen, R. K. Mishra, J. Li and A. M. Minor, *Nano Lett.*, 2012, **12**, 887-892.
51. L. Lu, Y. Shen, X. Chen, L. Qian and K. Lu, *Science*, 2004, **304**, 422-426.
52. S. Sun, D. Deng, C. Kong, X. Song and Z. Yang, *Dalton Trans.*, 2012, **41**, 3214-3222.
53. M. Liu, L. Wang, G. Lu, X. Yao and L. Guo, *Energy Environ. Sci.*, 2011, **4**, 1372-1378.
54. L. Ruan, E. Zhu, Y. Chen, Z. Lin, X. Huang, X. Duan and Y. Huang, *Angew. Chem. Int. Ed.*, 2013, **52**, 12577-12581.
55. S. Acharya, S. Sarkar and N. Pradhan, *Phys. Chem. Lett.*, 2012, **3**, 3812-3817.
56. Y. Zhang, Y. Tang, X. Liu, Z. Dong, H. H. Hng, Z. Chen, T. C. Sum and X. D. Chen, *Small*, 2013, **9**, 996-1002.
57. J. R. Ran, J. Zhang, J. Yu, M. Jaroniec and S. Z. Qiao, *Chem. Soc. Rev.*, 2014, **43**, 7787-7812.
58. J. Liu, G. K. Zhang, J. C. Yu and Y. D. Guo, *Dalton Trans.*, 2013, **42**, 5092-5099
59. Z. R. Shen, S. T. Sun, W. J. Wang, J. W. Liu, Z. F. Liu and J. C. Yu, *J. Mater. Chem. A*, 2015, DOI:10.1039/c4ta06871h.
60. L. Shang, T. Bian, B. Zhang, D. Zhang, L.-Z. Wu, C.-H. Tung, Y. D. Yin and T. R Zhang, *Angew. Chem. Int. Ed.*, 2014, **53**, 250-254.
61. V. R. Stamenkovic, B. Fowler, B. S. Mun, G. Wang, P. N. Ross, C. A. Lucas and N. M. Marković, *Science*, 2007, **315**, 493-497.
62. K. Yoon, Y. Yang, P. Lu, D. Wan, H.-C. Peng, K. Stamm Masias, P. T. Fanson, C. T. Campbell and Y. Xia, *Angew. Chem. Int. Ed.*, 2012, **51**, 9543-9546.
63. P. Xu, R. Yu, H. Ren, L. Zong, J. Chen and X. Xing, *Chem. Sci.*, 2014, **5**, 4221-4226.



 